

Goal-Oriented Influence-Maximizing Data Acquisition for Learning and Optimization

Weichi Yao
University of Michigan
weichiy@umich.edu

Bianca Dumitrascu
Columbia University
bmd2151@columbia.edu

Bryan R. Goldsmith
University of Michigan
bgoldsm@umich.edu

Yixin Wang
University of Michigan
yixinw@umich.edu

February 24, 2026

Abstract

Active data acquisition is central to many learning and optimization tasks in deep neural networks, yet remains challenging because most approaches rely on predictive uncertainty estimates that are difficult to obtain reliably. To this end, we propose Goal-Oriented Influence-Maximizing Data Acquisition (GOIMDA), an active acquisition algorithm that avoids explicit posterior inference while remaining uncertainty-aware through inverse curvature. GOIMDA selects inputs by maximizing their expected influence on a user-specified goal functional, such as test loss, predictive entropy, or the value of an optimizer-recommended design. Leveraging first-order influence functions, we derive a tractable acquisition rule that combines the goal gradient, training-loss curvature, and candidate sensitivity to model parameters. We show theoretically that, for generalized linear models, GOIMDA approximates predictive-entropy minimization up to a correction term accounting for goal alignment and prediction bias, thereby, yielding uncertainty-aware behavior without maintaining a Bayesian posterior. Empirically, across learning tasks (including image and text classification) and optimization tasks (including noisy global optimization benchmarks and neural-network hyperparameter tuning), GOIMDA consistently reaches target performance with substantially fewer labeled samples or function evaluations than uncertainty-based active learning and Gaussian-process Bayesian optimization baselines.

Keywords: Deep learning, Active acquisition, Bayesian optimization, Active learning, Influence function

1 Introduction

Active data acquisition is central to many learning and optimization problems in science and engineering, where evaluations or labels are costly, and budgets are limited. A prominent example arises in materials science, where the goal is to discover materials with exceptional properties defined over a vast design space of elemental compositions and atomic structures [1, 2]. Evaluating a single candidate typically requires material synthesis followed by experimental testing, making each function evaluation expensive and time-consuming.

Similar challenges appear in biological system identification, where researchers seek to characterize the response of a system to external stimuli [3]. In this setting, a predictive model—often a neural network—is trained on existing stimulus–response pairs and used to guide the selection of new stimuli that are expected to reduce prediction error. Each new response, however, must be obtained through complex laboratory experiments, making data acquisition the primary bottleneck.

A third example is hyperparameter optimization for deep neural networks [4]. Hyperparameters govern both model architecture and training dynamics and have a large impact on performance. Evaluating a single configuration requires a full training and validation cycle, which is computationally expensive, especially for large-scale models.

Across these domains, the common challenge is to optimize a task-specific objective using as few evaluations as possible. A natural approach is iterative data acquisition: starting from an initial dataset \mathcal{D} (which can be empty), one repeatedly fits a model \mathcal{M} to the current data and selects the next input x to evaluate by maximizing an acquisition function $a(x)$ that estimates the expected utility of labeling x .

When neural networks are used as the underlying model, most existing approaches, spanning Bayesian optimization and deep active learning, rely on predictive uncertainty to guide data selection. For example, in materials design and hyperparameter tuning, Bayesian optimization methods often use posterior predictive uncertainty to balance exploration and exploitation [5, 6], while in stimulus–response learning, uncertainty-based criteria dominate active learning practice [7–10]. Uncertainty estimates therein are typically obtained via Bayesian neural networks [11] or ensemble-based methods [5–7, 9].

Despite their popularity, reliable uncertainty estimation for deep neural networks remains a major challenge. Exact Bayesian inference is intractable, and approximate methods are often computationally expensive, sensitive to modeling choices, and poorly calibrated in high-dimensional regimes [11–13]. As a result, uncertainty-driven acquisition functions can be unreliable or impractical, limiting their effectiveness in modern deep learning pipelines.

Main idea. To address this challenge, we propose *Goal-Oriented Influence-Maximizing Data Acquisition (GOIMDA)*, an iterative acquisition algorithm that is uncertainty-aware without explicit posterior inference. Rather than quantifying predictive uncertainty, GOIMDA selects data points based on their expected *influence* on a user-specified *goal objective function* of the model parameters.

The goal can represent diverse scientific objectives, such as test loss, predictive entropy, or the value of an optimizer-recommended design. In other words, GOIMDA maximizes a goal objective function while minimizing data acquisition efforts.

Using first-order influence functions, we derive a tractable acquisition rule that combines (i) the gradient of the goal objective, (ii) an inverse-curvature preconditioner given by the inverse Hessian of the empirical training loss, and (iii) each candidate’s sensitivity to the model parameters. The goal gradient and candidate sensitivity promote goal-directed exploitation by favoring points whose induced parameter updates are most aligned with directions that improve the goal. At the same time, the inverse curvature term acts as a local uncertainty proxy that encourages exploration by prioritizing updates in directions the current data constrains the least. This yields an exploration–exploitation trade-off without maintaining a Bayesian posterior [14–17].

More formally, let (x, y) denote a feature–label pair with $x \in \mathcal{X}$ and $y \in \mathcal{Y}$, and let $p_0(y | x)$ be the unknown data-generating conditional distribution. We assume that sampling inputs x is free, while observing labels y is costly. Let \mathcal{M}_θ be a supervised model of $p_\theta(y | x)$ with parameters θ , trained by minimizing the negative log-likelihood loss

$$\ell(\theta; (x, y)) = -\log p_\theta(y | x).$$

The goal objective function \mathcal{G} can be flexibly defined for various scientific tasks that can be formulated as optimization problems. Without loss of generality, the following discussion focuses on minimizing \mathcal{G} . We consider the goal objective function \mathcal{G} as a function of θ , which parametrizes and reflects the best knowledge of the unknown distribution p_0 .

Goal-Oriented Influence-Maximizing Data Acquisition alternates between two steps:

1. At each step, we fit a model $p_\theta(y | x)$ with model parameters θ by minimizing the empirical risk function on the existing data set \mathcal{D}

$$\theta(\mathcal{D}) = \arg \min_{\theta} \frac{1}{|\mathcal{D}|} \sum_{(u,v) \in \mathcal{D}} \ell(\theta; (u, v)). \quad (1)$$

2. We choose to label the next data point that maximizes the expected influence \mathcal{I} of any candidate x on the goal objective function \mathcal{G}

$$x_{\text{next}} = \arg \max_x \mathbb{E}_y [\mathcal{I} \circ \mathcal{G}(\theta(\mathcal{D} \cup \{(x, y)\}))], \quad (2)$$

where the influence is measured by the instantaneous rate at which upweighting x gives the maximum change in \mathcal{G}

$$\mathcal{I} \circ \mathcal{G}(\theta(\mathcal{D} \cup \{(x, y)\})) := s \cdot \frac{\partial}{\partial \epsilon} \mathcal{G}(\theta^\epsilon(\mathcal{D} \cup \{(x, y)\})) \Big|_{\epsilon=0}, \quad (3)$$

where

$$s = \begin{cases} +1, & \text{maximization of } \mathcal{G} \\ -1, & \text{minimization of } \mathcal{G} \end{cases}.$$

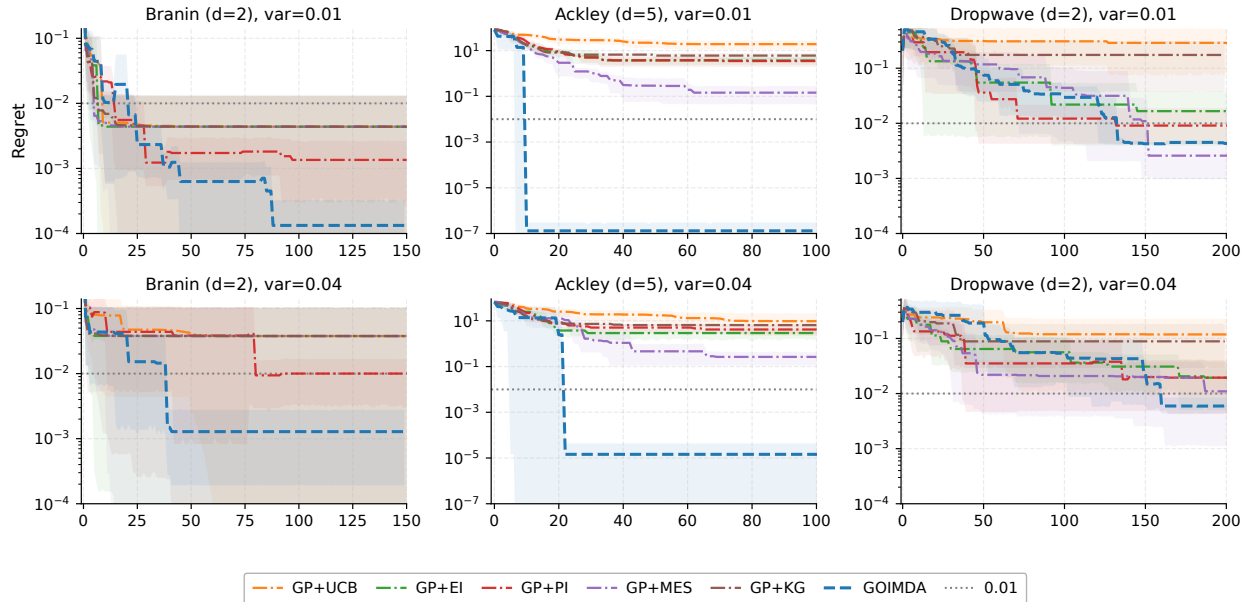


Figure 1: GOIMDA reaches lower immediate regret with fewer acquisitions than Bayesian optimization baselines on noisy objective functions. The Bayesian optimization baselines are Gaussian Processes-based with acquisition functions: upper confidence bound (GP+UCB), expected improvement (GP+EI), probability of improvement (GP+PI), max-value entropy search (GP+MES), and knowledge gradient (GP+KG). Immediate regret is reported at each acquisition step for the Branin, Ackley, and Dropwave benchmarks under two noise levels ($\sigma^2 = 0.01, 0.04$). Solid/dashed curves show the mean performance across runs, and shaded regions denote bootstrapped 95% confidence intervals of the mean (computed across runs). Across all tasks, GOIMDA consistently achieves lower regret earlier in the acquisition process, with the advantage generally becoming more pronounced at higher noise levels.

In this formulation, $\theta^\epsilon(\mathcal{D} \cup \{(x, y)\})$ is the parameter estimate after x is added to the current dataset \mathcal{D} with weight ϵ , and the output of any candidate x is approximated using resampling techniques such as Jackknife [18].

Contributions. We introduce GOIMDA, a general active data acquisition framework that selects new queries by maximizing their expected first-order influence on a user-specified goal functional (e.g., test loss, predictive entropy, or the value of an optimizer-recommended design). We derive a tractable influence-based acquisition rule that couples the goal gradient, training-loss curvature (via inverse-Hessian-vector products), and candidate sensitivity. We provide a scalable implementation using a Jackknife/deep-ensemble surrogate to approximate unknown labels and stochastic inverse-Hessian vector product solvers to handle modern neural networks.

We further develop theoretical results under exponential-family models, showing that GOIMDA approximates predictive-entropy minimization up to a correction term that accounts for goal alignment and prediction bias. This result explains how GOIMDA captures uncertainty-related behavior through the same curvature structure that underlies predictive entropy, while modulating it via goal alignment and prediction bias, but without maintaining a posterior over θ .

Finally, we demonstrate empirically across a range of learning and optimization tasks, including image and text classification, noisy global optimization benchmarks, and neural-network hyperparameter tuning, that GOIMDA consistently achieves target performance with substantially fewer labeled samples or function evaluations than uncertainty-based active learning algorithms and Gaussian-process Bayesian optimization baselines. See Figure 1 for an example, where we benchmark GOIMDA on noisy black-box function optimization from [19] with five other commonly used Gaussian Processes (GP)-based Bayesian optimization methods with different acquisition functions, namely, probability of improvement (PI) [20], expected improvement (EI) [21], upper confidence bound (UCB) [22], max-value entropy search (MES) [23], and knowledge gradient (KG) [24–26]; more details provided in Section 5 for empirical studies.

Organization. The rest of the paper is organized as follows: Section 2 presents the GOIMDA algorithm and its scalable implementation. Section 3 develops theory under exponential-family models and connects GOIMDA to predictive-entropy-based acquisition. Section 5 reports empirical results on learning and optimization benchmarks. It concludes with a discussion of related work in Section 6, along with the scope and limitations in Section 7.

2 Goal-Oriented Influence-Maximizing Data Acquisition

We introduce *goal-oriented influence-maximizing data acquisition (GOIMDA)*. Unlike standard acquisition strategies that optimize proxy criteria (e.g., predictive uncertainty alone), GOIMDA allows the user to specify an explicit *goal objective*

$$\mathcal{G}(\theta(\mathcal{D})),$$

which encodes the scientific task of interest and depends on the model parameters $\theta(\mathcal{D})$ learned from the currently labeled dataset \mathcal{D} . At each iteration, the objective is to acquire the data point whose label is expected to yield the largest improvement in this goal.

A naïve implementation would retrain the model for every candidate x to evaluate the post-update value of \mathcal{G} , which is computationally infeasible. We therefore develop an *influence-function-based approximation*. Using classical influence functions, we estimate the *first-order change* in \mathcal{G} induced by infinitesimally upweighting a candidate example. This yields a tractable acquisition score that couples: (i) the goal gradient $\nabla_{\theta}\mathcal{G}$, (ii) a curvature preconditioner given by the inverse Hessian of the empirical training loss, and (iii) the candidate’s parameter sensitivity $\nabla_{\theta}\ell(\theta; (x, y))$.

To handle unknown candidate labels and to scale to modern neural networks, we further introduce (a) a surrogate ensemble to approximate expectations over unknown labels and (b) scalable implicit inverse–Hessian–vector products, avoiding explicit construction of H_{θ}^{-1} . The remainder of this section specifies representative goal objectives \mathcal{G} , derives the influence-function-based acquisition rule, and presents practical algorithms for efficient implementation.

2.1 Goal Objective Function

We consider the goal objective \mathcal{G} defined as a function of the current fitted parameters $\theta := \theta(\mathcal{D})$, which summarize the most up-to-date model induced by the acquired dataset \mathcal{D} . This formulation allows \mathcal{G} to be flexibly instantiated to match different scientific tasks.

Global optimization. Consider minimizing an unknown function f , whose observations take the form $y = f(x) + \epsilon$. This setting covers applications such as materials design and neural-network hyperparameter tuning. Let $x^* = \arg \min_x f(x)$ denote the true minimizer, which is unknown. We define the goal objective \mathcal{G} as

$$\mathcal{G}^{\text{opt}}(\theta) := \mathbb{E}_{y \sim p_0(\cdot | \hat{x}_\theta^*)} [y], \quad (4)$$

the expected property value at the model’s recommended minimizer \hat{x}_θ^* , obtained by minimizing model’s predictive mean $\mathbb{E}_{y \sim p_\theta(\cdot | x)} [y]$.

Targeted supervised learning. For supervised learning problems where performance is evaluated on an unlabeled target set \mathcal{U} that shares the same conditional distribution $p_0(y | x)$, we define \mathcal{G} as a utility function over \mathcal{U} . A common choice is the negative log-likelihood:

$$\mathcal{G}^{\text{nl}}(\theta) := - \sum_{x \in \mathcal{U}} \mathbb{E}_{y \sim p_0(\cdot | x)} [\log p_\theta(y | x)]. \quad (5)$$

When the objective places greater importance on reducing errors for hard or low-confidence predictions, as opposed to uniformly penalizing all examples, we adopt the focal loss [27]:

$$\mathcal{G}^{\text{foc}}(\theta) := - \sum_{x \in \mathcal{U}} \mathbb{E}_{y \sim p_0(\cdot | x)} [(1 - p_\theta(y | x))^\gamma \log p_\theta(y | x)], \quad (6)$$

where γ is a predefined focused parameter or the relaxation parameter.

Entropy-based objectives. If the goal is to reduce predictive uncertainty on \mathcal{U} , we use the Shannon entropy of the model’s predictive distribution:

$$\mathcal{G}^{\text{ent}}(\theta) := - \sum_{x \in \mathcal{U}} \mathbb{E}_{y \sim p_\theta(\cdot | x)} [\log p_\theta(y | x)]. \quad (7)$$

Although \mathcal{G}^{ent} and \mathcal{G}^{nl} share the same functional form, they differ in the underlying expectation: the former is taken with respect to the model distribution p_θ , while the latter is evaluated under the true conditional distribution p_0 .

Overall, these examples illustrate that the goal objective \mathcal{G} can be adapted to a wide range of tasks. Without loss of generality, we focus on settings where the objective is to *minimize* \mathcal{G} .

2.2 Influence Function

2.2.1 Goal-based informativeness

Given a goal minimization objective \mathcal{G} , we call a candidate input x_c *informative* if acquiring its label is expected to affect the model update and hence reduce \mathcal{G} the most.

Intuitively, a candidate data point is informative if its inclusion would substantially alter the learned model parameters and, as a result, lead to a significant reduction in the goal objective. This notion is formalized below.

Definition 1 (Informativeness). *Given a goal objective \mathcal{G} and a current dataset \mathcal{D} , the informativeness of a candidate input x_c is measured by the change in the goal objective after adding x_c to \mathcal{D} :*

$$\Delta\mathcal{G} := \mathcal{G}(\theta(\mathcal{D} \cup \{(x_c, y_c)\})) - \mathcal{G}(\theta(\mathcal{D})). \quad (8)$$

Here, $\theta(\mathcal{D})$ and $\theta(\mathcal{D} \cup \{(x_c, y_c)\})$ denote the parameters before and after acquiring x_c , respectively.

Although this definition is conceptually clear, directly evaluating $\Delta\mathcal{G}$ is computationally infeasible, as it requires retraining the model for every candidate x_c and every possible label y_c . In the following, we introduce an influence-function-based approximation [28] that enables efficient estimation of informativeness without retraining the model.

2.2.2 Influence function approximation

We define the influence of a candidate point (x_c, y_c) on the goal objective \mathcal{G} as the instantaneous change in \mathcal{G} induced by infinitesimally upweighting this point in the training objective; see (3). In the case of minimizing the goal objective \mathcal{G} , the influence defined takes the instantaneous rate with a negative sign

$$\mathcal{I} \circ \mathcal{G}(\theta(\mathcal{D} \cup \{(x_c, y_c)\})) = - \left. \frac{\partial}{\partial \epsilon} \mathcal{G}(\theta^\epsilon(\mathcal{D} \cup \{(x_c, y_c)\})) \right|_{\epsilon=0}, \quad (9)$$

where $\theta^\epsilon(\mathcal{D} \cup \{(x_c, y_c)\})$ is the parameter estimate when x_c is added to \mathcal{D} with weight ϵ :

$$\theta^\epsilon(\mathcal{D} \cup \{(x_c, y_c)\}) = \arg \min_{\theta} \frac{1}{|\mathcal{D}|} \sum_{(u,v) \in \mathcal{D}} \ell(\theta; (u, v)) + \epsilon \ell(\theta; (x_c, y_c)). \quad (10)$$

Maximizing the influence score for maximizing informativeness. The following result shows that maximizing the reduction in \mathcal{G} when candidate x_c is added in the training set \mathcal{D} can be linearly approximated by maximizing $\mathcal{I} \circ \mathcal{G}(\theta(\mathcal{D} \cup \{(x_c, y_c)\}))$ without retraining the model.

Proposition 2. *The influence score of a candidate point (x_c, y_c) on the goal minimization objective \mathcal{G} , defined in (9), approximates the reduction in \mathcal{G} after adding x_c to \mathcal{D} .*

Proof. By definition of $\Delta\mathcal{G}$ in (8), $\Delta\mathcal{G}$ is negative for minimization of the goal objective \mathcal{G} . To maximize the reduction in \mathcal{G} , we maximize $-\Delta\mathcal{G}$. Since applying the first-order Taylor expansion on the goal objective function $\mathcal{G}(\theta^\epsilon(\mathcal{D} \cup \{(x_c, y_c)\}))$ at $\epsilon = 0$ gives

$$\mathcal{G}(\theta^\epsilon(\mathcal{D} \cup \{(x_c, y_c)\})) = \mathcal{G}(\theta(\mathcal{D})) + \left[\left. \frac{\partial}{\partial \epsilon} \mathcal{G}(\theta^\epsilon(\mathcal{D} \cup \{(x_c, y_c)\})) \right] \Big|_{\epsilon=0} \cdot \epsilon + o(\epsilon^2), \quad (11)$$

we have

$$-\Delta\mathcal{G} \approx - \frac{1}{|\mathcal{D}|} \left[\left. \frac{\partial}{\partial \epsilon} \mathcal{G}(\theta^\epsilon(\mathcal{D} \cup \{(x_c, y_c)\})) \right] \Big|_{\epsilon=0} \stackrel{(9)}{=} \frac{1}{|\mathcal{D}|} \mathcal{I} \circ \mathcal{G}(\theta(\mathcal{D} \cup \{(x_c, y_c)\})). \quad (12)$$

Therefore, we can linearly approximate the reduction in test loss due to adding x_c without retraining the model by computing $\frac{1}{|\mathcal{D}|} \mathcal{I} \circ \mathcal{G}$. \square

Under a minimization objective, the most informative data point is the one that induces the greatest reduction in the goal objective. Proposition 2 shows that the reduction can be linearly approximated via the influence score. As a result, selecting the most informative data point reduces to choosing the candidate with the maximum influence [29]. In this precise sense, the influence-score-based acquisition criterion is well justified: it corresponds to the greedy choice that most effectively decreases \mathcal{G} under a first-order influence approximation.

2.2.3 Closed-form influence score

We now derive a closed-form expression for the influence score, which yields a tractable acquisition criterion. The explicit form of (9) can be derived by first applying the chain rule:

$$\mathcal{I} \circ \mathcal{G}(\theta(\mathcal{D} \cup \{(x_c, y_c)\})) = - \left[\nabla_{\theta} \mathcal{G}(\theta(\mathcal{D})) \right]^{\top} \cdot \left[\frac{\partial}{\partial \epsilon} \theta^{\epsilon}(\mathcal{D} \cup \{(x_c, y_c)\}) \right] \Big|_{\epsilon=0}, \quad (13)$$

To evaluate the parameter sensitivity term, we apply standard influence-function arguments. Using the first-order optimality condition of $\theta^{\epsilon}(\mathcal{D} \cup \{(x_c, y_c)\})$ and the fact that $\theta^{\epsilon}(\mathcal{D} \cup \{(x_c, y_c)\}) \rightarrow \theta(\mathcal{D})$ as $\epsilon \rightarrow 0$ [30], a classical Taylor expansion on $\frac{\partial}{\partial \epsilon} \theta^{\epsilon}(\mathcal{D} \cup \{(x_c, y_c)\})$ in (13) at $\epsilon = 0$ gives

$$\frac{\partial}{\partial \epsilon} \theta^{\epsilon}(\mathcal{D} \cup \{(x_c, y_c)\}) \Big|_{\epsilon=0} \approx - H_{\theta}^{-1} \left[\nabla_{\theta} \ell(\theta; (x_c, y_c)) \right] \Big|_{\theta=\theta(\mathcal{D})}, \quad (14)$$

where H_{θ} is the Hessian matrix

$$H_{\theta} := \frac{1}{|\mathcal{D}|} \sum_{(u,v) \in \mathcal{D}} \nabla_{\theta}^2 \ell(\theta; (u, v)). \quad (15)$$

Substituting (14) into (13) yields a closed-form approximation $\tilde{\mathcal{I}} \circ \mathcal{G}(\theta(\mathcal{D} \cup \{(x_c, y_c)\}))$ for (13). Since the candidate label y_c is unknown at acquisition time, we take expectation with respect to the true conditional distribution $p_0(y | x_c)$, obtaining the expected influence score

$$\mathbb{E}_{y_c \sim p_0(\cdot | x_c)} \left[\tilde{\mathcal{I}} \circ \mathcal{G}(\theta(\mathcal{D} \cup \{(x_c, y_c)\})) \right] = \left[\nabla_{\theta} \mathcal{G}(\theta(\mathcal{D})) \right]^{\top} H_{\theta}^{-1} \left[\nabla_{\theta} \mathbb{E}_{y_c \sim p_0(\cdot | x_c)} \ell(\theta; (x_c, y_c)) \right] \Big|_{\theta=\theta(\mathcal{D})}. \quad (16)$$

Equation (16) provides an explicit, first-order approximation to the influence of a candidate point on the goal objective \mathcal{G} , without requiring access to the retrained parameters $\theta(\mathcal{D} \cup \{(x_c, y_c)\})$. Consequently, the most informative candidate can be selected by maximizing (16). This yields an efficient goal-oriented data acquisition rule that directly targets reductions in \mathcal{G} while avoiding the computational cost of retraining the model for every candidate.

2.3 Practical and Scalable Implementation

By definition, the influence score in (9) with a closed-form expression (16) traces how the optimization of the goal objective \mathcal{G} propagates through the learned parameters θ and back to individual training data points, thereby identifying the point with the greatest potential to reduce \mathcal{G} . Proposition 2 further shows that maximizing the influence score provides an efficient approximation to maximizing the informativeness in terms of reduction in \mathcal{G} .

However, computing the closed-form influence score in (16) is nontrivial. First, evaluating the influence of any candidate input on the goal objective typically requires expectations over the true conditional distribution $p_0(y | x)$, which is unavailable in practice. Second, as the number of acquired data points $|\mathcal{D}|$ grows, directly computing the inverse Hessian H_θ^{-1} defined in (15) becomes prohibitively expensive, making naive influence-based acquisition infeasible. In this section, we introduce practical and scalable algorithms that address both challenges and enable efficient computation of the influence function in (16).

Approximating the unknown output variable. Goal objectives $\mathcal{G}(\theta)$ are often defined on unknown target outputs, such as (4) for iterative global optimization and (5) for active learning. At the same time, the influence score is evaluated at $\theta(\mathcal{D} \cup \{(x_c, y_c)\})$, where the candidate output y_c is unknown prior to acquisition. Consequently, computing the influence score of any candidate x_c requires an approximation of the goal objective \mathcal{G} with potentially unknown target outputs and the corresponding output y_c .

Most existing work that applies influence functions to iterative data acquisition operates within an active learning framework [31, 32]. One line of work selects goal objectives, such as negative prediction entropy (7) or variants of the Fisher Information Ratio [33], which depend only on the current model p_θ and do not explicitly target the test performance under the true data-generating distribution [31]. Another approach derives acquisition functions from upper bounds on the test loss, leading to criteria based on the gradient norm $\|\nabla_\theta \mathbb{E}_{y_c \sim p_\theta(\cdot|x_c)}[\ell(\theta; (x_c, y_c))]\|$ [32]. In both cases, the unknown candidate outputs y_c are approximated using the current model posterior p_θ , relying solely on training information.

In contrast, our objective is to directly optimize goal functions defined under the unknown true distribution p_0 , such as test loss in active learning or the minimal value in iterative global optimization. To this end, we approximate the unknown output without relying on the posterior of the primary model p_θ .

Specifically, we introduce a surrogate model $\tilde{\mathcal{M}}_\phi$ with model parameter ϕ , implemented as an ensemble of r neural networks with different random initializations and trained on different subsets of the training data. This approach is closely related to deep ensembles, which have been shown to improve predictive accuracy, uncertainty estimation, and robustness to distributional shift [34]. To further enhance predictive stability, we employ the Jackknife resampling technique [18]. Each ensemble member is trained on a Jackknife subsample of the available data, and the surrogate model outputs the average prediction across all r networks. The resulting Jackknife estimation has computational complexity $O(rm)$, where m is the number of model parameters.

Computing the inverse Hessian–vector product. Evaluating (16) requires computing the inverse of the Hessian matrix defined in (15). For a model \mathcal{M} with m trainable parameters and a dataset \mathcal{D} of size n , explicitly forming and inverting the Hessian incurs a computational cost of $O(nm^2 + m^3)$, which is infeasible for modern neural networks with millions of parameters.

To avoid explicit Hessian inversion, we approximate inverse Hessian–vector products (HVPs), which can be computed in linear time with respect to the number of parameters using automatic differentiation frameworks such as PyTorch and JAX. A common approach is to use conjugate

Algorithm 1 Goal-Oriented Influence-Maximizing Data Acquisition

Input: The initial data set \mathcal{D}

- 1: **repeat**
 - 2: Update both main model \mathcal{M}_θ and the ensemble model $\tilde{\mathcal{M}}_\phi$ on \mathcal{D}
 - 3: Select $x_{\text{next}} \leftarrow \arg \max_x \mathbb{E}_{y \sim p_\phi(\cdot|x)} [\tilde{\mathcal{I}} \circ \mathcal{G}_\phi(\theta(\mathcal{D} \cup \{(x, y)\}))]$ {see approximation in (18)}
 - 4: Query $y_{\text{next}} \leftarrow \text{OBSERVE}(x_{\text{next}})$
 - 5: Augment $\mathcal{D} \leftarrow \mathcal{D} \cup \{(x_{\text{next}}, y_{\text{next}})\}$
 - 6: **until** termination condition is met {e.g. budget exhausted or desired goal achieved}
-

gradient (CG) methods [35], which solve

$$\min_u u^\top (H^2 + \lambda I)u - (Hv)^\top u,$$

where the solution u^* approximates $H^{-1}v$. With L CG iterations, the computational cost is $O(nL)$, and in practice, convergence can often be achieved with a small number of iterations [36].

When the training dataset is very large, the linear dependence on n can still be costly. Alternatively, we adopt the LiSSA algorithm [37], which recursively estimates the inverse HVPs via

$$\hat{H}_j^{-1}v = v + (I - H)\hat{H}_{j-1}^{-1}v, \quad \hat{H}_0^{-1}v = v.$$

LiSSA stochastically approximates inverse HVPs using mini-batches of data at each iteration. With batch size B and L iterations, the computational complexity is $O(nm + BLm)$. Both CG and LiSSA are well-suited to large-scale settings with limited memory, and empirically, we observe no significant difference between them in terms of acquisition performance.

Goal-Oriented Influence-Maximizing Data Acquisition (GOIMDA): A general efficient iterative acquisition algorithm. In practice, we select the next acquisition point by

$$x_{\text{next}} = \arg \max_{x_c} \mathbb{E}_{y_c \sim p_\phi(\cdot|x_c)} [\tilde{\mathcal{I}} \circ \mathcal{G}_\phi(\theta(\mathcal{D} \cup \{(x_c, y_c)\}))], \quad (17)$$

where the influence term admits the explicit approximation

$$\tilde{\mathcal{I}} \circ \mathcal{G}_\phi(\theta(\mathcal{D} \cup \{(x_c, y_c)\})) = \left[\nabla_\theta \mathcal{G}_\phi(\theta(\mathcal{D})) \right]^\top \hat{H}_\theta^{-1} \left[\nabla_\theta \ell(\theta; (x_c, y_c)) \right] \Big|_{\theta=\theta(\mathcal{D})}. \quad (18)$$

Here, \mathcal{G}_ϕ denotes the goal objective approximated using the surrogate model $\tilde{\mathcal{M}}_\phi$ with model parameter ϕ in the absence of direct access to p_0 , and \hat{H}_θ^{-1} denotes a stochastic approximation of the inverse Hessian obtained via implicit HVPs. See Algorithm 1 for the complete algorithm.

3 Theoretical Properties of GOIMDA under Exponential Family Models

In this section, we study goal-oriented influence-maximizing data acquisition (GOIMDA) under exponential family models. We first formalize the exponential-family setting and derive GOIMDA in closed form. We then provide a geometric interpretation of the resulting influence function, clarify the role of the bias term, and compare GOIMDA with predictive-entropy-based acquisition.

Our study reveals that GOIMDA decomposes naturally into three interacting components: (i) *goal alignment*, captured by the gradient $\nabla_{\theta}\mathcal{G}$; (ii) *curvature preconditioning*, governed by the inverse Hessian H_{θ}^{-1} of the *empirical training loss*; and (iii) a *prediction-bias term* that quantifies the discrepancy between the model and the true data-generating mechanism. Together, these components define an acquisition criterion that is *uncertainty-aware in a local, curvature-based sense*: the inverse-curvature term prioritizes candidates that induce updates along parameter directions that are not yet well constrained by the current data.

For canonical Generalized Linear Models (GLMs), we make this connection explicit by showing that GOIMDA inherits the same H_{θ}^{-1} leverage factor that appears in predictive-entropy acquisition, while reweighted by goal alignment and prediction bias. Moreover, we derive a parameter-space surrogate for the bias term that replaces the unknown true conditional distribution with an estimable parameter discrepancy, yielding a fully tractable acquisition rule.

Overall, these results position GOIMDA as an *exploration-aware, bias-focused improvement surrogate*: it targets regions that are both influential for the goal and informative about model misspecification, without requiring a posterior distribution over θ .

Model setup. Let $x \in \mathbb{R}^d$ and $y \in \mathbb{R}$. We model the conditional distribution $y \sim p_{\theta}(\cdot | x)$ using an exponential family of the form

$$p_{\theta}(y | x) = h(y) \exp\left(\eta_{\theta}(x) T(y) - A(\eta_{\theta}(x))\right), \quad (19)$$

where $T(y)$ is the sufficient statistic and $\eta_{\theta}(x)$ is the natural parameter, parameterized by θ .¹ Exponential family distributions enjoy several well-known statistical properties:

(3.1) the log-partition function $A(\eta)$ is convex;

(3.2) $\mathbb{E}_{\eta}[T(y)] = A'(\eta)$;

(3.3) $\text{var}_{\eta}[T(y)] = A''(\eta)$.

In this setting, the natural parameter $\eta_{\theta}(x)$ is modeled by a deep neural network with parameters θ , trained via the negative log-likelihood loss $\ell(\theta; (x, y)) := -\log p_{\theta}(y | x)$, explicitly,

$$\ell(\theta; (x, y)) = -\log h(y) - \eta_{\theta}(x) T(y) + A(\eta_{\theta}(x)). \quad (20)$$

Influence score. Using the loss definition for $\ell(\theta; (x, y))$ in (20), the gradient of the expected loss at a candidate input x_c under the true data-generating distribution $p_0(\cdot | x_c)$ is given by

$$\nabla_{\theta} \mathbb{E}_{y_c \sim p_0(\cdot | x_c)} [\ell(\theta; (x_c, y_c))] = \nabla_{\theta} \eta_{\theta}(x_c) [A'(\eta_{\theta}(x_c)) - A'(\eta_0(x_c))].$$

Substituting this expression into the closed-form influence score (16) yields the following goal-oriented influence (GOI) score:

$$\text{GOI}(x_c) = [\nabla_{\theta} \mathcal{G}(\theta)]^{\top} H_{\theta}^{-1} \nabla_{\theta} \eta_{\theta}(x_c) [A'(\eta_{\theta}(x_c)) - A'(\eta_0(x_c))]. \quad (21)$$

¹We do not explicitly distinguish between scalar and vector-valued parameters in the notation.

When $T(y) = y$, the term $A'(\eta_\theta(x_c)) - A'(\eta_0(x_c))$ in (21) reduces to $\mathbb{E}_\theta[y | x_c] - \mathbb{E}_0[y | x_c]$, which corresponds to the *prediction bias* at x_c . Consequently, the next point to acquire is selected as

$$x_{\text{next}} = \arg \max_{x_c} \text{GOI}(x_c).$$

Geometric interpretation of the influence function. The acquisition criterion in (21) selects the candidate whose *curvature-aware* parameter perturbation is most aligned with the direction that maximally decreases \mathcal{G} , while prioritizing regions where the model is currently biased.

Define $\mu := H_\theta^{-1/2} \nabla_\theta \mathcal{G}(\theta)$, $\nu(x_c) := H_\theta^{-1/2} \nabla_\theta \eta_\theta(x_c)$, and $b(x_c) := A'(\eta_\theta(x_c)) - A'(\eta_0(x_c))$. With these definitions, the goal-oriented influence score can be written as

$$\text{GOI}(x_c) = \underbrace{\langle \mu, \nu(x_c) \rangle}_{\substack{\text{goal alignment} \\ \text{in the } H_\theta\text{-geometry}}} \times \underbrace{b(x_c)}_{\substack{\text{prediction bias} \\ \mathbb{E}_\theta[y|x_c] - \mathbb{E}_0[y|x_c]}}, \quad (22)$$

where the first factor quantifies how strongly a curvature-aware update in the direction suggested by x_c is expected to decrease \mathcal{G} , and then the second factor gates this directional effect by the magnitude of the local predictive bias.

Concretely, μ acts as a sensitivity vector that encodes which parameter directions matter for improving \mathcal{G} , whereas $\nu(x_c)$ characterizes the candidate's induced update direction after accounting for local curvature. The preconditioning by H_θ^{-1} transforms Euclidean gradients into second-order-aware directions, down-weighting parameter components that are already well-determined by existing data and amplifying directions where the model remains uncertain or weakly identified; this yields an approximately reparameterization-invariant notion of alignment and prioritizes candidates that can meaningfully refine the model in parts that are not yet well determined. Finally, the multiplicative bias factor $b(x_c)$ converts this leverage in parameter space into expected improvement of the goal. That is, if the model is already well-calibrated at x_c then $b(x_c) \approx 0$ and the predicted first-order gain is negligible, whereas a larger $|b(x_c)|$ steers acquisition toward regions where the predictive mean deviates from the data-generating process and parameter updates translate into tangible reductions of \mathcal{G} .

The bias term. To obtain a tractable approximation of the bias term, we apply a first-order Taylor expansion of $A'(\eta_0(x_c))$ around $\theta_0 = \theta$, yielding

$$A'(\eta_\theta(x_c)) - A'(\eta_0(x_c)) \approx \nabla_\theta \eta_\theta(x_c)^\top (\theta - \theta_0) A''(\eta_\theta(x_c)). \quad (23)$$

Substituting this approximation into (22) gives

$$\text{GOI}(x_c) = \underbrace{\langle \mu, \nu(x_c) \rangle}_{\substack{\text{goal alignment} \\ \text{in the } H\text{-geometry}}} \times \underbrace{\nabla_\theta \eta_\theta(x_c)^\top (\theta - \theta_0)}_{\text{directional parameter bias at } x_c} A''(\eta_\theta(x_c)). \quad (24)$$

which makes the dependence on the *parameter bias* $\theta - \theta_0$ explicit.

The geometric decomposition in (22) highlights *prediction bias* at the output level through the discrepancy in predictive means. In contrast, the approximation in (24) replaces the unobservable term $A'(\eta_0)$ with the estimable *parameter bias* $(\theta - \theta_0)$. This re-expression attributes bias to

concrete directions in parameter space via $\nabla_{\theta}\eta_{\theta}(x)$ and recovers the familiar structure of GLMs, where $b(x) \approx A''(\eta_{\theta}(x))x^{\top}(\theta - \theta_0)$. This form will be leveraged in the subsequent comparison with predictive-entropy-based acquisition.

Connection to predictive entropy (PE) minimization. The most widely used acquisition criteria in active learning are uncertainty-based. In contrast, influence-maximizing acquisition does not explicitly require uncertainty estimates of the predictive model \mathcal{M}_{θ} . For neural networks, such uncertainty estimates are often computationally expensive to obtain and unreliable in the early stages of data acquisition, when the training set is small.

Despite this apparent difference, there is a close connection between influence maximization and predictive entropy minimization in Bayesian GLMs. In particular, for GLMs with a canonical link, influence maximization can be interpreted as an approximation to predictive entropy minimization, as formalized in Proposition 3.

Proposition 3. *Influence maximization approximates predictive entropy minimization in GLMs with a canonical link. Under mild assumptions, the two objectives differ by an additional term that calibrates the directional parameter bias up to a constant.*

Proof. Consider a generalized linear model in the form of (19) with a canonical link $\eta_{\theta}(x) = x^{\top}\theta$ and $T(y) = y$. The conditional entropy of model after acquiring (x_c, y_c) can be derived as

$$\mathcal{H}(\theta \mid \mathcal{D} \cup \{(x_c, y_c)\}) = \frac{1}{2} \mathbb{E}_{y_c \sim p_0(\cdot \mid x_c)} [\log |H_{\theta_c}^{-1}|] + \text{const} \quad (25)$$

where H_{θ_c} is the Hessian of negative log likelihood with model parameter $\theta_c = \theta(\mathcal{D} \cup \{(x_c, y_c)\})$.

Under the canonical-link assumption and properties (3.2) and (3.3), minimizing (25) can be simplified to minimize [38]

$$\mathbb{E}_{y_c \sim p_0(\cdot \mid x_c)} [\log |H_{\theta_c}^{-1}|] = \log |H_{\theta}^{-1}| - \log \left(1 + x_c^{\top} H_{\theta}^{-1} x_c A''(\eta_{\theta}(x_c)) \right). \quad (26)$$

Denote $z = x_c^{\top} H_{\theta}^{-1} x_c A''(\eta_{\theta}(x_c))$. Given that $A''(\eta_{\theta}(x_c))$ is bounded and $x_c^{\top} H_{\theta}^{-1} x_c \rightarrow 0$ as $|\mathcal{D}| \rightarrow \infty$ [39], if z is sufficiently small, the standard linear approximation $\log(1 + z) = z + o(z)$ further simplifies the acquisition objective function as

$$\text{PE}(x_c) := -x_c^{\top} H_{\theta}^{-1} x_c A''(\eta_{\theta}(x_c)). \quad (27)$$

On the other hand, the acquisition score under GOIMDA (24) is

$$\text{GOI}(x_c) := [\nabla_{\theta} \mathcal{G}(\theta)]^{\top} H_{\theta}^{-1} x_c \underbrace{x_c^{\top} (\theta - \theta_0)}_{\text{prediction bias}} A''(\eta_{\theta}(x_c)), \quad (28)$$

where the additional directional parameter bias term coincides with the prediction bias under the context of GLMs with a canonical link.

By comparing objective in (27) with the one in (28), GOIMDA differs by multiplicative *goal-alignment* and *bias* weights:

$$\text{GOI}(x_c) \propto \text{PE}(x_c) \cdot \frac{\langle H_{\theta}^{-1/2} \nabla_{\theta} \mathcal{G}(\theta), H_{\theta}^{-1/2} x_c \rangle}{\|H_{\theta}^{-1/2} x_c\|^2} \cdot [x_c^{\top} (\theta - \theta_0)]. \quad (29)$$

This observation indicates that GOIMDA implicitly calibrates model uncertainty. The only distinction is that GOIMDA weights each parameter dimension according to its current bias, whereas predictive entropy minimization treats all dimensions uniformly. \square

Proposition 3 shows that, for canonical GLMs, GOIMDA inherits the same H_θ^{-1} leverage structure $A''(\eta_\theta(x_c)) x_c^\top H_\theta^{-1} x_c$ that underlies predictive-entropy selection. Crucially, GOIMDA *calibrates* this uncertainty signal through two additional factors: (i) a *goal-alignment* term that projects parameter updates onto the descent direction of \mathcal{G} , and (ii) a *prediction-bias* term that emphasizes inputs where the model disagrees with the data-generating mechanism.

As a result, GOIMDA is *uncertainty-aware*; it preserves the predictive-entropy signal, while actively steering acquisition toward directions that most effectively reduce the stated goal and toward regions of systematic error, all without requiring a posterior distribution over θ .

Consequently, although GOIMDA is derived as a goal-directed influence maximization procedure and is therefore inherently exploitative, it remains *exploration-aware*: it preferentially scores candidates in high-leverage, high-variance regions, thereby implicitly encouraging exploration. This should be distinguished from Bayesian exploration, which integrates over a posterior on θ ; here, $\theta(\mathcal{D})$ is held fixed.

In active learning, where prediction calibration is rarely made explicit, the bias term focuses acquisition on misfit or systematically mislabeled regions. Empirically, the results in Section 5.1 show that incorporating this bias achieves target accuracy with substantially fewer labels than omitting it, confirming that *calibrating bias materially improves sample efficiency*. In global optimization, GOIMDA plays the role of an *exploration-aware, exploitation-focused* alternative that mirrors the exploitation component of Bayesian optimization without requiring a posterior.

4 Example Applications of GOIMDA

We instantiate the GOIMDA framework for three representative use cases: *global optimization of noisy functions*, where the goal is to identify the minimizer of a complex, expensive-to-evaluate objective under noise; *hyperparameter tuning*, where the aim is to achieve optimal test performance while minimizing the number of costly training-and-validation evaluations; and *deep active learning*, where the objective is to train a classification model that generalizes well using as few labeled samples as possible.

Owing to the flexibility of the user-defined goal objective function, GOIMDA applies naturally across a wide range of problem settings. As introduced in Section 2, the goal objective can be defined to address global optimization problems involving black-box objectives that lack analytical expressions and do not admit first- or second-order derivatives; see (4). We also presented the goal functions tailored to deep active learning, where the objective is to optimize performance on a validation or test set under a limited labeling budget; see (5) and (7).

In this section, we focus on exponential family models to illustrate how GOIMDA can be instantiated in practice for both global optimization and active learning. For each example, we first specify the corresponding goal objective \mathcal{G} , and then derive the resulting influence-function-based acquisition rule (17) used in Algorithm 1.

4.1 Example Application I: Iterative Global Optimization with Noisy Observations

We consider a global optimization problem of the form $x_{\min} = \arg \min_x f(x)$ for an unknown objective function f . Direct evaluations of f are unavailable; instead, we observe noisy function values $y = f(x) + \varepsilon$, where ε is zero-mean noise. At each iteration, model \mathcal{M}_θ with parameters $\theta := \theta(\mathcal{D})$ is trained on the currently acquired dataset $\mathcal{D} = \{(u_i, v_i)\}_{i=1}^n$ to approximate the underlying function f .

We define the goal objective \mathcal{G} as in (4), the expected value of the true function at the model's recommended minimizer. Under the exponential family assumption with $T(y) = y$, this objective can be written as

$$\mathcal{G}(\theta) := \mathbb{E}_{y \sim p_0(\cdot | \hat{x}_\theta^*)}[y] \stackrel{(3.2)}{=} A'(\eta_0(\hat{x}_\theta^*)), \quad (30)$$

with the model's recommended minimizer

$$\hat{x}_\theta^* = \arg \min_x \mathbb{E}_{y \sim p_\theta(\cdot | x)}[y]. \quad (31)$$

By construction, GOIMDA selects the candidate whose acquisition yields the largest *instantaneous expected decrease* in the true objective evaluated at the model's current recommendation.

The gradient of the goal objective with respect to θ follows from the chain rule:

$$\nabla_\theta \mathcal{G}(\theta) := A''(\eta_0(\hat{x}_\theta^*)) \left[\frac{\partial}{\partial \theta} \hat{x}_\theta^* \right] [\nabla_x \eta_0(\hat{x}_\theta^*)]. \quad (32)$$

The derivative $\frac{\partial}{\partial \theta} \hat{x}_\theta^*$ can be obtained via implicit differentiation of the optimality conditions defining \hat{x}_θ^* (see Appendix A for details), yielding the approximation

$$\frac{\partial}{\partial \theta} \hat{x}_\theta^* \approx \left[\frac{\partial^2}{\partial \theta \partial x} A'(\eta_\theta(\hat{x}_\theta^*)) \right] [\nabla_x^2 A'(\eta_\theta(\hat{x}_\theta^*))]^{-1}. \quad (33)$$

Substituting these expressions into the influence function (21) yields the following explicit decomposition of the Goal-Oriented Influence score:

$$\text{GOI}(x_c) = \underbrace{A''(\eta_0(\hat{x}_\theta^*)) \nabla_x \eta_0(\hat{x}_\theta^*)^\top}_{\substack{\text{how the true objective drops} \\ \text{if } \hat{x}_\theta^* \text{ moves}}} \underbrace{\left[\nabla_x^2 A'(\eta_\theta(\hat{x}_\theta^*)) \right]^{-1} \left[\frac{\partial^2}{\partial \theta \partial x} A'(\eta_\theta(\hat{x}_\theta^*)) \right]}_{\substack{\text{how } \hat{x}_\theta^* \text{ moves when } \theta \text{ moves}}} \underbrace{H_\theta^{-1} \nabla_\theta \eta_\theta(x_c) b(x_c)}_{\substack{\text{how } \theta \text{ moves} \\ \text{when adding } (x_c, y_c)}, \quad (34)$$

where $b(x_c) := A'(\eta_\theta(x_c)) - A'(\eta_0(x_c))$ denotes the prediction-bias term introduced in (22).

In practice, the unknown true natural parameter $\eta_0(\cdot)$ is approximated using a Jackknife resampling strategy with the deep ensemble model $\tilde{\mathcal{M}}_\phi$, and inverse HVPs are computed stochastically, as described in Section 2.

4.2 Example Application II: Hyperparameter Optimization

We next consider hyperparameter tuning for neural networks under a transfer learning setup, which induces a more complex optimization problem. Hyperparameters determine the model architecture and training configuration, and different choices of hyperparameters typically lead to different trained parameters and, consequently, different test performance. Evaluating even a single hyperparameter configuration requires training and validating a neural network, which is computationally expensive. The goal is therefore to identify hyperparameters that yield strong test performance while minimizing the number of costly training and validation runs.

Formally, let $\xi \in \Xi$ denote the hyperparameters of a model trained on a fixed training dataset $\mathcal{D}^{\text{tr}} = \{(x_i^{\text{tr}}, y_i^{\text{tr}})\}_{i=1}^n$, and let $(x, y) \in \mathcal{X} \times \mathcal{Y}$ denote a test input–output pair, where y may be unobserved.² Denote the predictive test negative log-likelihood loss obtained by a model trained with hyperparameters ξ as $h_0(x, \xi)$, which depends on both the test input x and the hyperparameters ξ . Due to stochastic effects such as random initialization and optimization noise, repeated training with the same ξ can yield different validation outcomes. As a result, we only observe noisy evaluations of h_0 in its noisy form, $r = h_0(x, \xi) + \varepsilon$, where ε denotes observation noise. The goal is to optimize h_0 with respect to ξ given x , as the “mean” test performance is indifferent to stochastic variability in the model training.

Let $q_0(\cdot \mid x, \xi)$ denote the true conditional distribution of the noisy observation r given the concatenated input (x, ξ) , parameterized by θ_0 . We train a model with parameters θ on the currently acquired dataset \mathcal{D} , whose elements take the form $([x, \xi], r)$. Under the exponential family assumption, the likelihood is

$$q_\theta(r \mid x, \xi) = h(r) \exp\left(\eta_\theta(x, \xi) T(r) - A(\eta_\theta(x, \xi))\right). \quad (35)$$

The search for the set of hyperparameters that yields optimal expected test performance is then formulated via the goal objective

$$\mathcal{G}(\theta) := \mathbb{E}_{r \sim q_0(\cdot \mid x, \hat{\xi}_\theta^*)}[r], \quad (36)$$

where $\hat{\xi}_\theta^*$ denotes the minimizer of model \mathcal{M}_θ ’s predictive test negative log-likelihood loss

$$\hat{\xi}_\theta^* = \arg \min_{\xi} \mathbb{E}_{r \sim q_\theta(\cdot \mid x, \xi)}[r]. \quad (37)$$

The formulation in (36) mirrors the iterative global optimization with noisy observations in (30), with the decision variable specialized to hyperparameters for fixed test inputs. Consequently, the influence score for hyperparameter acquisition can be derived analogously to (34).

4.3 Example Application III: Deep Active Learning

We illustrate how Goal-Oriented Influence-Maximizing Data Acquisition (GOIMDA) can be applied to deep active learning under exponential family distributions. We first define a test-centric goal objective function $\mathcal{G}(\theta)$ and then derive a closed-form *influence score* for adding a candidate (x_c, y_c) . The resulting acquisition criterion couples the H_θ^{-1} geometry with a *prediction-bias* weighting.

²For ease of exposition, we consider a single test input x .

Formally, consider a classification task where $x \in \mathbb{R}^d$ denotes the input features and $y \in \mathbb{Z}$ denotes the output label. This setting also captures the motivating biological example, where x corresponds to experimental stimuli and y to the measured system response, and where conducting experiments to read the system response is costly. At each iteration, a deep neural network \mathcal{M}_θ with parameters $\theta := \theta(\mathcal{D})$ is trained on the currently labeled dataset \mathcal{D} to model the conditional distribution of the response y given the stimuli x . Test inputs (x, y) are drawn from the same unknown data-generating distribution p_0 , with y unobserved at acquisition time.

The objective of active learning is to iteratively select inputs x_{next} for label acquisition such that the model achieves low test loss $\ell(\theta; (x, y))$ using as few labeled samples as possible.

To optimize the model performance on test data (x, y) where y is unknown, a natural test-centric goal objective is

$$\mathcal{G}(\theta) := \mathbb{E}_{y \sim p_0(\cdot|x)} [\ell(\theta; (x, y))]. \quad (38)$$

Using the explicit exponential-family loss in (20), the gradient of \mathcal{G} takes the form

$$\nabla_\theta \mathcal{G}(\theta) = [A'(\eta_\theta(x)) - A'(\eta_0(x))] \nabla_\theta \eta_\theta(x). \quad (39)$$

Substituting this expression into the influence function (21) yields the influence score for a candidate x_c :

$$\begin{aligned} \text{GOI}(x_c) &= [A'(\eta_\theta(x)) - A'(\eta_0(x))] \nabla_\theta \eta_\theta(x)^\top H_\theta^{-1} \nabla_\theta \eta_\theta(x_c) [A'(\eta_\theta(x_c)) - A'(\eta_0(x_c))] \\ &\propto \nabla_\theta \eta_\theta(x)^\top H_\theta^{-1} \nabla_\theta \eta_\theta(x_c) [A'(\eta_\theta(x_c)) - A'(\eta_0(x_c))], \end{aligned} \quad (40)$$

where the proportionality follows by discarding terms independent of x_c . Consequently, the next point to acquire is

$$x_{\text{next}} = \arg \max_{x_c} \nabla_\theta \eta_\theta(x)^\top H_\theta^{-1} \nabla_\theta \eta_\theta(x_c) [A'(\eta_\theta(x_c)) - A'(\eta_0(x_c))]. \quad (41)$$

Under the canonical-link assumption with $T(y) = y$, this expression simplifies to

$$x_{\text{next}} = \arg \max_{x_c} x_c^\top H_\theta^{-1} x_c \underbrace{x_c^\top (\theta - \theta_0)}_{\text{prediction bias}} A''(\eta_\theta(x_c)), \quad (42)$$

which recovers (28) with the goal objective defined in (38) for the active learning setting.

In practice, the prediction-bias term is estimated using a Jackknife resampling strategy via the deep ensemble surrogate $\tilde{\mathcal{M}}_\phi$, and inverse HVPs are computed stochastically (see Section 2).

5 Empirical Studies

We empirically evaluate GOIMDA on a diverse set of controlled and realistic learning and optimization tasks.³ We begin with a synthetic logistic-regression study designed to isolate the effect of the parameter-bias term in the acquisition rule. Next, we evaluate GOIMDA for noisy global optimization of black-box test functions, benchmarking against standard Gaussian-process Bayesian

³Code to reproduce our experiments is available at github.com/weichiyao/GOIMDA.

optimization methods with common acquisition functions [20–24]. We also apply GOIMDA to hyperparameter tuning on CIFAR-10 under distribution shift, where the goal is to select hyperparameters that improve performance on a target test distribution using labels only from a different source distribution. Finally, we study predictive learning on image and text classification benchmarks [40–42], comparing GOIMDA against uncertainty-based active learning baselines such as BALD [43–45].

5.1 On the importance of the parameter-bias term in (24)

The approximation in (24) makes the dependence on the parameter bias $\theta - \theta_0$ explicit. This parameter-bias form is useful in two ways. Conceptually, it attributes prediction bias to specific parameter directions via $\nabla_{\theta}\eta_{\theta}(x)$, which supports diagnostics and motivates targeted regularization. Computationally, it enables a plug-in implementation using Jackknife/Bootstrap surrogates of θ_0 , requiring a single solve for $H_{\theta}^{-1}\nabla_{\theta}\mathcal{G}$ and per-candidate vector–Jacobian (or Jacobian–vector) products. Hence, the parameter-bias form is both interpretable and computationally practical.

In canonical GLMs (Proposition 3), GOIMDA shares the same H_{θ}^{-1} leverage structure as predictive-entropy selection; the key difference is GOIMDA’s bias calibration, which re-weights parameter directions by their current bias instead of treating them uniformly. In particular, apart from goal alignment, the additional factor is the prediction-bias term $x_c^{\top}(\theta - \theta_0)$. If $\theta - \theta_0$ is replaced by a vector of ones, the influence objective (28) reduces to the predictive-entropy objective (27) up to a scaling constant, recovering a bias-agnostic leverage rule.

To quantify the practical importance of $\theta - \theta_0$, we run a controlled simulation that compares acquisition variants based on (28). Inputs $x \in \mathbb{R}^d$ are generated from a low-rank latent-variable model $z \in \mathbb{R}^l, l < d$ [46]: $x = Wz + \epsilon$, with $z \sim \mathcal{N}(0, I)$ and $\epsilon \sim \mathcal{N}(0, \sigma^2 I)$. We set $d = 20, l = 3$, and $\sigma = 0.1$. Outcomes are binary with $p_0(y | x)$ given by a Bernoulli GLM. For each of 200 repetitions, we generate 50,000 training points and 5,000 test points. At each acquisition step, we refit logistic regression on the labeled set and select the next point by maximizing (28) under different treatments of the bias term; random pool sampling serves as a baseline. All runs start from two labeled points (one per class), and the remaining training points form the candidate pool. Test accuracy is recorded after each acquisition.

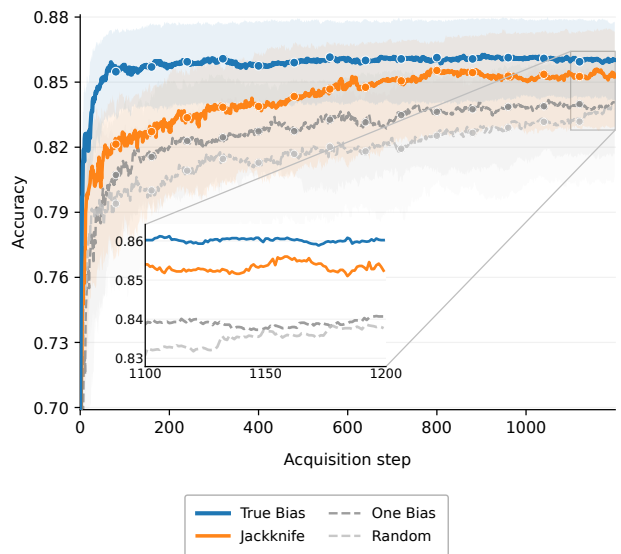


Figure 2: The parameter-bias term is crucial for effective data acquisition, and a good approximation significantly improves the acquisition performance. Using the true bias term (blue) reaches high accuracy with fewer acquisitions, and a principled approximation (orange) outperforms ignoring the bias term (dark gray dashed). The inset zoom highlights the persistent gap. Shaded regions indicate variability across runs. Test accuracy is shown versus the number of acquired labels (averaged over 200 repetitions). Higher is better.

Figure 2 compares four acquisition strategies including (i) *True Bias*: influence maximization using the true bias term $\theta - \theta_0$; (ii) *Jackknife*: influence maximization using a Jackknife estimate of $\theta - \theta_0$; (iii) *One Bias*: influence maximization with $\theta - \theta_0$ replaced by a vector of ones; and (iv) *Random*: random acquisition from the pool.

As expected, *True Bias* reaches high accuracy with the fewest acquisitions, and *Jackknife* closely tracks it. *One Bias* still improves over random sampling but consistently lags behind the bias-aware variants. Overall, ignoring the bias term reduces acquisition efficiency: the better we approximate $\theta - \theta_0$, the faster accuracy improves, and the fewer labels are required.

5.2 Noisy black-box function optimization

We benchmark GOIMDA on noisy Branin, Drop-Wave, and Ackley functions, the black-box test functions from [19], where each query returns $y = f(x) + \varepsilon$ with $\varepsilon \sim \mathcal{N}(0, \sigma^2)$. We consider $\sigma \in \{0.1, 0.2\}$ and start each run with 5 initial observations. See full details in Appendix B.1.

Figure 1 provides a performance comparison on 2D Branin and 5D Ackley functions between GOIMDA and five other commonly used Gaussian Processes (GP)-based Bayesian optimization methods with different acquisition functions. In each of these plots, we show the *immediate regret*, which measures the difference between the outcome of the best possible decision ($\min_{x \in \mathcal{S}} f(x)$ for some feasible set \mathcal{S}) and the outcome of the decision made by each active optimization method. Given its noisy nature, the regret value may go up in consecutive acquisition steps, but should, in general, decline if solved by an effective optimization algorithm.

Across all three benchmarks, GOIMDA (blue dashed) reduces immediate regret much faster than the GP baselines, typically reaching the lowest regret within the first few dozen acquisitions and then stabilizing. On Branin, GOIMDA quickly drops below the other methods for both noise levels; when noise increases from $\sigma^2 = 0.01$ to $\sigma^2 = 0.04$, the GP baselines plateau at noticeably higher regret while GOIMDA maintains a substantially lower plateau, widening the gap. On Ackley, the contrast is even sharper: GOIMDA rapidly drives regret down by orders of magnitude, whereas other GP baselines improve slowly and remain far above GOIMDA throughout; this separation persists and effectively becomes more pronounced under the higher noise setting. On Dropwave, all methods are more competitive, but GOIMDA still achieves the lowest or near-lowest regret earlier, and the advantage becomes clearer at $\sigma^2 = 0.04$, where increased noise slows the baselines more than GOIMDA. Overall, higher noise degrades all methods, but GOIMDA is markedly more noise-robust, retaining rapid early gains and a lower final regret.

5.3 Hyperparameter tuning under distribution shift

We study hyperparameter optimization when training labels are available only from a labeled source distribution (X, Y) , but performance is evaluated on an unlabeled target distribution under distribution shift (\tilde{X}, \tilde{Y}) with unknown \tilde{Y} . The marginals p_X and $p_{\tilde{X}}$ may differ, while the conditional model is assumed to share the same form $p_{\theta_0} := p_{\theta_0}(Y | X)$ for unknown θ_0 .

Concretely, we instantiate this setting on CIFAR-10 with a Pre-Activation ResNet backbone. We construct an imbalanced labeled source set and an unlabeled target set drawn from a restricted set of classes. Full details of the dataset construction and splits can be found in Appendix B.2.

In this setting, hyperparameter selection is driven only by source training/validation performance can favor configurations that fit the imbalanced source distribution, but transfer poorly to the target distribution. GOIMDA instead evaluates hyperparameters by their estimated influence on the expected prediction loss on the target distribution, while still leveraging the labeled source data for training.

Figure 3 shows that GOIMDA consistently identifies hyperparameter settings that improve target performance under distribution shift more reliably than Bayesian optimization baselines. Measured by the Δ test regret relative to the initial configuration (step 0), GOIMDA quickly attains a stable negative improvement after only a few acquisitions and maintains the best mean regret across subsequent steps. In contrast, the Bayesian optimization baselines exhibit larger variance and less consistent progress, often oscillating around smaller improvements and occasionally reverting toward worse target performance; this indicates that optimizing based on source-driven signals can select configurations that do not transfer well. Overall, the results suggest that explicitly scoring candidates by their estimated influence on target loss makes hyperparameter search more sample-efficient and robust to distribution shift.

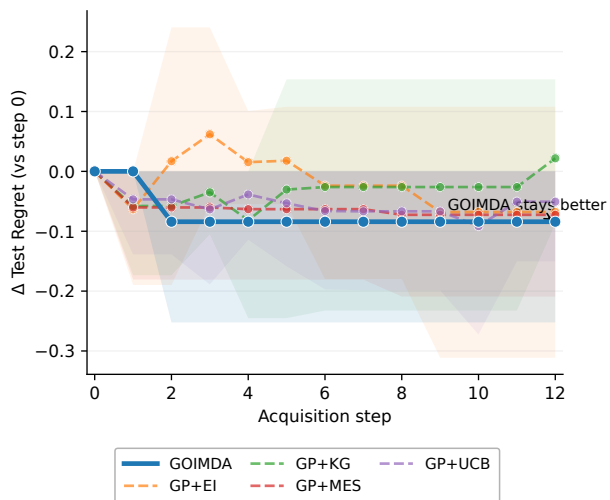


Figure 3: GOIMDA selects the hyperparameters that provide the best prediction performance on the target test set compared to Bayesian optimization methods. The performance is evaluated in terms of the Δ test regret relative to the initial configuration (step 0) across acquisition steps. Solid line shows GOIMDA; dashed lines show Bayesian optimization baselines. Shaded regions indicate 95% bootstrap confidence intervals of the mean across 3 trials. Negative values correspond to improved target-set performance.

5.4 Predictive learning

We evaluate GOIMDA in standard active learning loops: at each iteration, the model is trained on the current labeled set and then selects the next point from a pool \mathcal{S} . Across datasets, we use comparable feedforward architectures (stacked linear-relu layers followed by softmax) for all methods. BALD adds dropout layers and uses MC dropout for approximate inference [44]. All models are trained with Adam [47] (learning rate 0.001, $\beta_1 = 0.9$, $\beta_2 = 0.999$) on a single GPU. Test accuracy is measured after each acquisition. Results are aggregated over four independent trials; error bars show the mean and the lower/upper quartiles.

We consider three benchmarks spanning image and text classification: MNIST [40], EMNIST Letters [41], and binary sentiment classification derived from the Rotten Tomatoes phrase dataset [48]. For each benchmark, we follow a standard pool-based protocol with a small balanced initialization, a held-out validation set, and the remaining training points as the acquisition pool; see Appendix B.3 for exact split sizes and preprocessing choices.

Table 1: GOIMDA requires fewer samples than BALD and random acquisition to achieve high accuracy on MNIST. The table reports 25%-, 50%-, and 75%-percentiles for the number of required data points to reach 80%, 90%, and 95% accuracy on MNIST. Higher is better.

% Accuracy	Acquisition Methods		
	GOIMDA	BALD	Random
80%	88/108/116	104/109/117	138/150/173
90%	374/422/441	432/445/475	846/901/977
95%	1060/1150/1206	1514/1589/1678	4265/4522/4731

MNIST We follow the standard protocol of [44] with a small balanced initial labeled set and a fixed validation hold-out; remaining points form the pool (see Appendix B.3.1 for more details). GOIMDA and Random acquisitions are assessed with an architecture of three linear-relu layers with hidden widths 392 and 128. BALD uses a similar architecture with two linear-dropout-relu layers followed by the final linear-softmax output layer, with the same hidden unit dimensions. We use 100 MC dropout samples in BALD. The expected loss for the test data points and that for candidate data points in GOIMDA are approximated using 10 Jackknife samples.

EMNIST Letters We follow a similar pool/validation setup as in MNIST (see Appendix B.3.2 for more details). Similar to what is used in MNIST, GOIMDA, and Random have three linear-relu layers with hidden unit dimensions 392 and 128, respectively, and BALD adds two additional dropout layers for inference. In addition, 50 MC dropout samples are used in BALD for acquisition. To compute the expected loss for the test data points and the expected loss for candidate data points, 5 Jackknife samples are used to approximate the expected loss in GOIMDA.

Movie reviews (Rotten Tomatoes) For the Rotten Tomatoes dataset, we form a binary task by mapping the original 5-level sentiment labels into $\{0, 1\}$ after removing neutral phrases, then apply a bag-of-words preprocessing pipeline; see full details in Appendix B.3.3. The initial training set contains a balanced dataset of size 20. GOIMDA and Random have three linear-relu layers with hidden unit dimensions 64 and 64, respectively. BALD again adds two additional dropout layers for inference. In addition, 50 MC dropout samples are used in BALD for acquisition. To compute the expected loss for the test data points and the expected loss for candidate data points, 10 Jackknife samples are used to approximate the expected loss in GOIMDA.

Table 1 and Figure 4 show that GOIMDA is consistently more sample-efficient than BALD and random acquisition. On MNIST, GOIMDA reaches high accuracy with much fewer labeled examples—often requiring only a small fraction of the labeling budget needed by random sampling—highlighting the value of targeted acquisition. The learning curves in Figure 4 reinforce this trend, with GOIMDA maintaining the highest test accuracy throughout the acquisition process. On EMNIST Letters, GOIMDA again achieves the best performance, delivering a clear accuracy advantage over both BALD and random, while BALD provides only marginal improvement over

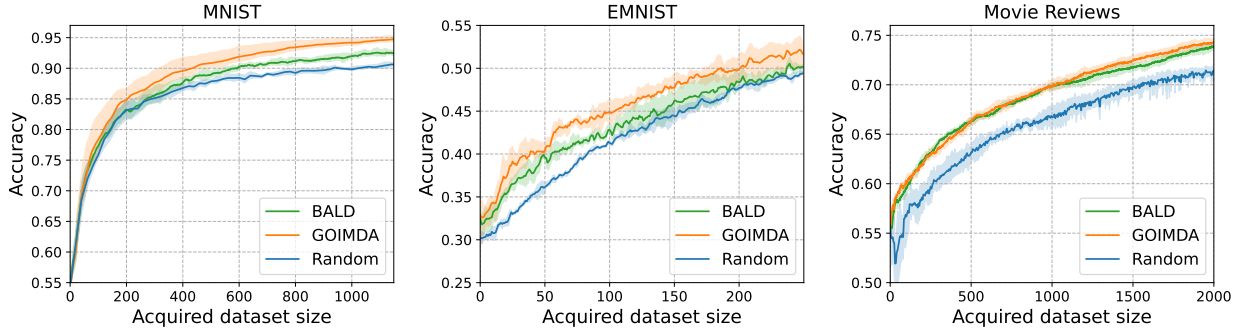


Figure 4: GOIMDA outperforms both random acquisition and BALD on classification tasks on images of digits from MNIST (Left) and EMNIST (Middle), and the sentiment of movie reviews from the Rotten Tomatoes dataset (Right). The test accuracy is evaluated at each acquisition step. Left: GOIMDA outperforms both random acquisition and BALD on MNIST. Middle: GOIMDA outperforms both random acquisition and BALD on EMNIST, whereas BALD only performs slightly better than random acquisition. Right: Both GOIMDA and BALD outperform the random sampling in terms of the accuracy rate at a given acquired dataset size. While GOIMDA and BALD have similar performance, GOIMDA gives slightly higher accuracy rates after the total acquisition size reaches 1,000.

random acquisition. On Movie Reviews, GOIMDA and BALD both outperform random sampling at essentially every acquisition step, with GOIMDA matching or slightly exceeding BALD; the tighter uncertainty bands for GOIMDA/BALD also suggest more stable gains than random selection.

6 Related work

This work draws on three themes around iterative data acquisition under expensive evaluation or labeling costs.

6.1 Iterative data acquisition for optimization

A standard approach to solving expensive black-box optimization problems is iterative data acquisition, in which a surrogate model is often fit to observed evaluations, and an acquisition function is used to select new inputs [49–52]. The most influential instantiation of this paradigm is *Bayesian optimization* (BO) [5, 6, 53], which maintains a probabilistic surrogate \mathcal{M} of the unknown objective and selects new evaluations by optimizing an acquisition function that balances exploration and exploitation.

Classical BO methods typically rely on Gaussian process (GP) surrogates [54] together with acquisition criteria such as Probability of Improvement (PI) [20, 55], Expected Improvement (EI) [21, 56], Upper Confidence Bound (UCB) [22], Entropy Search (ES) [57, 58], Max-value Entropy Search (MES) [23], and Knowledge Gradient (KG) [4, 24–26, 59].

Despite its empirical success, BO exhibits several practical limitations [5, 6, 52, 53]. First, GP-based surrogates require forming and factorizing an $n \times n$ kernel matrix at each iteration, incurring $\mathcal{O}(n^2)$ memory and $\mathcal{O}(n^3)$ time complexity [52, 54]. This rapidly becomes prohibitive as the

number of evaluations grows. To address scalability or high-dimensional settings, prior work has proposed structured or high-dimensional GP variants, low-dimensional embeddings, and localized trust-region methods such as TuRBO [60–65]. While effective in some regimes, these approaches often impose restrictive modeling assumptions, introduce additional posterior-maintenance overhead, and can be sensitive to model miscalibration [6, 66]. Second, replacing GPs with more scalable surrogates—such as tree- or density-based models [67, 68] or Bayesian neural networks [12, 69]—can alleviate computational costs, but frequently at the expense of uncertainty calibration or robustness [11, 66]. Third, many acquisition functions require expectations under the surrogate’s posterior predictive distribution. Fully Bayesian treatments, involving hyperparameter marginalization and exact acquisition computation, are rarely tractable in practice. Consequently, BO typically relies on plug-in hyperparameter estimates [21, 64] or Monte Carlo approximations [4, 12, 59, 69, 70], which respectively forgo proper marginalization and introduce additional computational overhead and estimator variance [11, 52, 53, 66, 71].

Motivated by these challenges, we pursue an alternative that avoids explicit posterior inference altogether. The proposed GOIMDA algorithm scores candidate points by the first-order effect that upweighting them would have on a task-level objective. This yields an exploration-aware yet bias-focused improvement strategy. Under exponential-family models, GOIMDA retains the inverse curvature and variance terms that underlie predictive-entropy-based acquisitions, thereby capturing uncertainty while modulating them through goal alignment and predictive bias to emphasize exploitation. As we show in subsequent sections, GOIMDA recovers the exploitation behavior of Bayesian optimization without maintaining a posterior, offering a practical alternative when Bayesian updates are computationally expensive or poorly calibrated [6, 52, 53].

6.2 Iterative data acquisition for learning

A closely related paradigm in supervised learning is *active learning* (AL), which aims to construct accurate predictive models using as few labeled examples as possible [7]. AL addresses supervised learning settings in which labeled data are expensive to obtain and the learner must adaptively decide which inputs to query. A canonical example arises in biological stimulus–response studies, where experimental cost limits the number of probes and careful selection of stimuli is crucial for learning accurate predictive models.

Here, we focus on AL for deep learning (DL) models, which have achieved remarkable success across domains due to their expressive representations and strong function-approximation capabilities. Most deep AL methods have been developed for classification tasks, particularly in image and text domains [8–10], and are also covered in broader surveys of active learning [7].

In pool-based deep AL, an *acquisition function* assigns a utility score to each unlabeled data point, and the learner queries those with the highest scores at each iteration. Existing acquisition strategies for deep neural networks can be broadly categorized into three families [9, 10]: (i) *uncertainty-based* methods, which query points about which the model is most uncertain [44, 45, 72–85]; (ii) *representation-based* methods, which select points that are prototypical or diverse in a learned feature space [86–96]; and (iii) *hybrid* methods, which combine uncertainty with

diversity or representativeness in feature or gradient space [97–108]. The latter two categories are particularly common in batch-mode acquisition, where the goal is to select a set of informative yet non-redundant points in each AL round.

Among these approaches, *uncertainty-based* criteria remain the most widely used in both classical and deep active learning [7, 8]. These methods are typically instantiated via confidence-, margin-, or entropy-based scores [73–75, 109, 110], Bayesian mutual-information objectives such as BALD and its batch extensions [44, 45, 72, 84], or expected model-change criteria that approximate loss reduction [31, 82, 111–113]. A recent work proposed to score candidate queries by how much they are expected to reduce predictive uncertainty on target inputs, making the acquisition objective directly aligned with downstream predictive performance [114]. In deep learning, these strategies commonly rely on approximate Bayesian neural networks (e.g., Monte Carlo dropout) [44, 115, 116] or deep ensembles [79, 80], and have also been combined with discriminative or energy-based scoring functions [80, 83, 85].

Despite their empirical success, uncertainty-based deep AL methods face fundamental challenges. Predictive probabilities from modern neural networks are often poorly calibrated, with models exhibiting overconfidence even when incorrect or under distribution shift [8, 117, 118]. Moreover, Bayesian neural networks require approximate inference procedures that are computationally expensive and can be unreliable in the small-data regimes typical of early AL rounds [13]. As highlighted in recent surveys, obtaining reliable and well-calibrated uncertainty estimates in deep models remains an open problem, which directly limits the robustness of uncertainty-driven deep active learning [8–10].

In contrast, GOIMDA avoids explicit posterior inference altogether while remaining uncertainty-aware. We build on influence functions as an alternative basis for data acquisition. Rather than explicitly modeling predictive uncertainty, influence-based methods estimate how upweighting a candidate point would affect the trained model or a downstream evaluation objective, without retraining from scratch [29]. By using influence scores for query selection, GOIMDA avoids reliance on calibrated uncertainty estimates while still implicitly capturing aspects of uncertainty and prediction bias. As we show in Section 3, under an exponential-family assumption, GOIMDA admits a connection to predictive entropy minimization: it retains uncertainty-sensitive inverse curvature terms while explicitly incorporating a prediction-bias component, resulting in an exploration-aware yet exploitation-focused acquisition rule.

6.3 Influence-function-based algorithms

Influence functions (IFs) originate in robust statistics as a principled tool for quantifying the infinitesimal effect of perturbing a data point on an estimator. Seminal work by Cook and colleagues developed a comprehensive diagnostic framework for identifying influential observations and assessing local influence in regression models, encompassing single-point and grouped perturbations, residual-based diagnostics, and empirical characterizations of influence [119–121].

These ideas were later revived in the deep-learning literature to analyze complex, nonconvex models. In particular, [29] demonstrated that first-order IFs can approximate the effect of upweighting or removing a training example on a model’s predictions, enabling practical tools for debugging, dataset curation, and attributing test errors to individual training points. Subsequent

work extended IFs to group-level effects [122], scalable approximations [123], higher-order and group influence [124, 125], and uncertainty quantification via higher-order IF and jackknife-style estimators [17]. More broadly, IF-based analyses have been used to uncover spurious data artifacts [126], characterize memorization and long-tail behavior [127], and study representational bias in neural networks [128].

Most existing applications of IFs in deep learning are retrospective: given a fixed, labeled training set—and often fixed test points—IFs are used to explain or diagnose existing predictions. In contrast, iterative data acquisition presents a fundamentally different setting. At selection time, the label of a candidate point is *unknown*, and acquisition must therefore be based on the *expected* influence of the candidate under a predictive distribution $p_0(y | x)$.

Prior work that leverages influence functions for iterative data acquisition has largely focused on active learning. An initial line of work proposes selecting data points based on their influence with respect to predefined utility functions [31, 129, 130]. These utility functions encode the learning “goal,” such as the training loss on an auxiliary labeled test set or predictive entropy computed from the current model. When test labels are unavailable, or when the candidate’s label is unknown, these methods rely on approximations using the current model p_θ , in the same spirit as standard uncertainty-based active learning. A related approach [32] avoids directly evaluating test loss by deriving an upper bound and selecting points based on the gradient norm of the candidate loss. However, terms involving unknown candidate outputs are again approximated using the current trained model alone.

Different from these works, we study the influence of a candidate data point on a *goal function* that is flexibly defined to cover a broad range of tasks. These include, for example, iterative optimization of black-box functions and label acquisition to improve performance on an unlabeled test set in active learning. Rather than approximating unknown quantities solely through the current trained model, we estimate them using a separate ensemble constructed via resampling techniques such as the jackknife. This decouples acquisition from a single potentially miscalibrated predictor and enables influence-based selection that remains effective when posterior uncertainty is expensive or unreliable to estimate.

7 Discussion

In this work, we introduce *Goal-Oriented Influence-Based Data Acquisition* (GOIMDA), a flexible iterative data acquisition algorithm that can be adapted to deep learning models over a wide range of tasks through user-defined, goal-oriented objective functions. By explicitly optimizing downstream objectives, GOIMDA enables active data acquisition to substantially reduce the number of required data points, leading to more efficient and cost-effective learning and optimization.

Several directions remain for future work. First, GOIMDA currently follows a fully sequential acquisition strategy, selecting a single data point at each iteration and updating the model immediately. While this approach maximizes data efficiency, it can increase overall training time. A natural acceleration strategy is to acquire batches of the top b points with the lowest individual influence scores. However, independent selection within a batch can reduce test performance due to redundancy and correlation among the acquired points, a limitation also observed in batch active

learning [44]. An important extension is therefore to account for interactions among candidate points—such as mutual information—in order to identify maximally influential acquisition batches while preserving computational efficiency.

Second, GOIMDA relies on supervised learning models as surrogates, using observed data to calibrate the current state of knowledge and to estimate both candidate responses and their impact on the target objective. Its effectiveness thus depends on the accuracy of these predictions for unseen data. Given the abundance of unlabeled information typically available in both candidate and target sets, integrating semi-supervised learning techniques may better capture the underlying structure of the feature space and further improve predictive performance. We leave the development of such semi-supervised extensions of GOIMDA to future work.

Acknowledgements. This work was supported in part by funding from the Office of Naval Research under grant N00014-23-1-2590, the National Science Foundation under grant No. 2310831, No. 2428059, No. 2435696, No. 2440954, a Michigan Institute for Data Science Propelling Original Data Science (PODS) grant, LG Management Development Institute AI Research, and Two Sigma Investments LP. Any opinions, findings, and conclusions or recommendations expressed in this material are those of the authors and do not necessarily reflect the views of the sponsors.

References

- [1] Turab Lookman, Prasanna V. Balachandran, Dezhen Xue, and Ruihao Yuan. Active learning in materials science with emphasis on adaptive sampling using uncertainties for targeted design. *npj Computational Materials*, 5(1):1–17, 2019.
- [2] Ghanshyam Paliana. Machine learning in materials science: From explainable predictions to autonomous design. *Computational Materials Science*, 193:110360, 2021.
- [3] Y. Sverchkov and M. Craven. A review of active learning approaches to experimental design for uncovering biological networks. *PLoS computational biology*, 13(6), 2017.
- [4] Jian Wu, Saul Toscano-Palmerin, P. Frazier, and Andrew Gordon Wilson. Practical multi-fidelity bayesian optimization for hyperparameter tuning. *ArXiv*, abs/1903.04703, 2019.
- [5] P. Frazier. A tutorial on bayesian optimization. *ArXiv*, abs/1807.02811, 2018.
- [6] Xilu Wang, Yaochu Jin, Sebastian Schmitt, and Markus Olhofer. Recent advances in bayesian optimization. *ACM Comput. Surv.*, 55(13s), 2023.
- [7] Burr Settles. Active learning literature survey. In *University of Wisconsin, Madison*, 2009. URL <https://api.semanticscholar.org/CorpusID:324600>.
- [8] Christopher Schröder and Andreas Niekler. A survey of active learning for text classification using deep neural networks. *ArXiv*, abs/2008.07267, 2020. URL <https://api.semanticscholar.org/CorpusID:221139929>.
- [9] Pengzhen Ren, Yun Xiao, Xiaojun Chang, Po-Yao Huang, Zihui Li, Brij B. Gupta, Xiaojiang Chen, and Xin Wang. A survey of deep active learning. *ACM Comput. Surv.*, 54(9), October 2021. ISSN 0360-0300. doi: 10.1145/3472291. URL <https://doi.org/10.1145/3472291>.
- [10] Dongyuan Li, Zhen Wang, Yankai Chen, Renhe Jiang, Weiping Ding, and Manabu Okumura. A survey on deep active learning: Recent advances and new frontiers. *IEEE Transactions on Neural Networks and Learning Systems*, 36(4):5879–5899, 2025. doi: 10.1109/TNNLS.2024.3396463.
- [11] Yucen Lily Li, Tim G. J. Rudner, and Andrew Gordon Wilson. A study of bayesian neural network surrogates for bayesian optimization. In *The Twelfth International Conference on Learning Representations*, 2024.
- [12] Jost Tobias Springenberg, Aaron Klein, Stefan Falkner, and Frank Hutter. Bayesian optimization with robust bayesian neural networks. In D. Lee, M. Sugiyama, U. Luxburg, I. Guyon, and R. Garnett, editors, *Advances in Neural Information Processing Systems*, volume 29. Curran Associates, Inc., 2016.
- [13] Julyan Arbel, Konstantinos Pitas, Mariia Vladimirova, and Vincent Fortuin. A primer on bayesian neural networks: Review and debates, 2023.
- [14] Bradley Efron. Frequentist accuracy of bayesian estimates. *Journal of the Royal Statistical Society: Series B (Statistical Methodology)*, 77(3):617–646, 2015.

- [15] Ryan Giordano, Tamara Broderick, and Michael I Jordan. Covariances, robustness, and variational bayes. *arXiv preprint*, abs/1709.02536, 2017.
- [16] Sanjib Basu, Sreenivasa Rao Jammalamadaka, and Wei Liu. Local posterior robustness with parametric priors: maximum and average sensitivity. In *Maximum Entropy and Bayesian Methods*, pages 97–106. Springer, 1996.
- [17] Ahmed Alaa and Mihaela Van Der Schaar. Discriminative jackknife: Quantifying uncertainty in deep learning via higher-order influence functions. In *International Conference on Machine Learning*, pages 165–174. PMLR, 2020.
- [18] John Tukey. Bias and confidence in not quite large samples. *Ann. Math. Statist.*, 29:614, 1958.
- [19] Derek Bingham. Optimization test functions. <http://www.sfu.ca/~ssurjano/ackley.html>, 2015.
- [20] A. Törn and A. Zilinskas. *Global optimization*, 1989.
- [21] Donald R. Jones, Matthias Schonlau, and William J. Welch. Efficient global optimization of expensive black-box functions. *Journal of Global Optimization*, 13(4):455–492, 1998.
- [22] N. Srinivas, A. Krause, S. Kakade, and M. Seeger. Gaussian process optimization in the bandit setting: No regret and experimental design. In *Proceedings of the 27th International Conference on International Conference on Machine Learning*, pages 1015–1022, 2010.
- [23] Zi Wang and Stefanie Jegelka. Max-value entropy search for efficient bayesian optimization. In *Proceedings of the 34th International Conference on Machine Learning*, volume 70, page 3627–3635. JMLR.org, 2017.
- [24] Warren Scott, Peter Frazier, and Warren Powell. The correlated knowledge gradient for simulation optimization of continuous parameters using gaussian process regression. *SIAM Journal on Optimization*, 21(3):996–1026, 2011.
- [25] Peter I. Frazier, Warren B. Powell, and Savas Dayanik. A knowledge-gradient policy for sequential information collection. *SIAM J. Control Optim.*, 47(5):2410–2439, 2008.
- [26] Peter I. Frazier, Warren B. Powell, and Savas Dayanik. The knowledge-gradient policy for correlated normal beliefs. *INFORMS Journal on Computing*, 21(4):599–613, 2009.
- [27] Tsung-Yi Lin, Priya Goyal, Ross Girshick, Kaiming He, and Piotr Dollár. Focal loss for dense object detection. *IEEE Transactions on Pattern Analysis and Machine Intelligence*, 42(2):318–327, 2020.
- [28] Peter J. Huber. The 1972 wald lecture robust statistics: A review. *The Annals of Mathematical Statistics*, 43(4):1041–1067, 1972.
- [29] Pang Wei Koh and Percy Liang. Understanding black-box predictions via influence functions. *arXiv preprint*, abs/1703.04730, 2017.
- [30] R. Dennis Cook and Sanford Weisberg. *Residuals and influence in regression*. Monographs on statistics and applied probability. Chapman and Hall, New York, 1982.

- [31] Minjie Xu and Gary Kazantsev. Understanding goal-oriented active learning via influence functions. *arXiv*, abs/1905.13183, 2019.
- [32] Tianyang Wang, Xingjian Li, Pengkun Yang, Guosheng Hu, Xiangrui Zeng, Siyu Huang, Cheng-Zhong Xu, and Min Xu. Boosting active learning via improving test performance. *arXiv*, abs/2112.05683, 2022.
- [33] Tong Zhang and Frank J. Oles. The value of unlabeled data for classification problems. In *International Conference on Machine Learning*, volume 20, page 1191–1198, 2000.
- [34] Stanislav Fort, Huiyi Hu, and Balaji Lakshminarayanan. Deep ensembles: A loss landscape perspective. *arXiv*, abs/1912.02757, 2020.
- [35] R.K. Mehra. Computation of the inverse hessian matrix using conjugate gradient methods. *Proceedings of the IEEE*, 57(2):225–226, 1969.
- [36] James Martens. Deep learning via hessian-free optimization. In *Proceedings of the 27th International Conference on International Conference on Machine Learning*, page 735–742, 2010.
- [37] Naman Agarwal, Brian Bullins, and Elad Hazan. Second-order stochastic optimization for machine learning in linear time. *The Journal of Machine Learning Research*, 18(1):4148–4187, 2017.
- [38] Jeremy Lewi, Robert Butera, and Liam Paninski. Efficient active learning with generalized linear models. In *Artificial Intelligence and Statistics*, pages 267–274, 2007.
- [39] Liam Paninski. Asymptotic theory of information-theoretic experimental design. *Neural Computation*, 17(7):1480–1507, 07 2005.
- [40] Yann LeCun, Corinna Cortes, and Christopher C. J. Burges. The mnist handwritten digit database. <http://yann.lecun.com/exdb/mnist/>, 1998.
- [41] Gregory Cohen, Saeed Afshar, Jonathan Tapson, and André van Schaik. Emnist: an extension of mnist to handwritten letters. *arXiv preprint arXiv:1702.05373*, 2017.
- [42] Kaggle. Sentiment analysis on movie reviews: Classify the sentiment of sentences from the rotten tomatoes dataset. <https://www.kaggle.com/c/sentiment-analysis-on-movie-reviews/data>, 2015.
- [43] Neil Houlsby, Ferenc Huszár, Zoubin Ghahramani, and Máté Lengyel. Bayesian active learning for classification and preference learning. *ArXiv*, abs/1112.5745, 2011.
- [44] Yarin Gal, Riashat Islam, and Zoubin Ghahramani. Deep bayesian active learning with image data. In *International Conference on Machine Learning*, pages 1183–1192. PMLR, 2017.
- [45] Andreas Kirsch, Joost van Amersfoort, and Yarin Gal. Batchbald: Efficient and diverse batch acquisition for deep bayesian active learning. In H. Wallach, H. Larochelle, A. Beygelzimer, F. d'Alché-Buc, E. Fox, and R. Garnett, editors, *Advances in Neural Information Processing Systems*, volume 32. Curran Associates, Inc., 2019.

- [46] Michael E. Tipping and Christopher M. Bishop. Probabilistic principal component analysis. *Journal of the Royal Statistical Society: Series B (Statistical Methodology)*, 61(3):611–622, 1999.
- [47] Diederik P Kingma and Jimmy Ba. Adam: A method for stochastic optimization. *arXiv preprint arXiv:1412.6980*, 2014.
- [48] Bo Pang and Lillian Lee. Seeing stars: Exploiting class relationships for sentiment categorization with respect to rating scales. In *Proceedings of the 43rd Annual Meeting of the ACL*, page 115–124, 2005.
- [49] A. J. Booker, J. E. Dennis, P. D. Frank, D. B. Serafini, V. Torczon, and M. W. Trosset. A rigorous framework for optimization of expensive functions by surrogates. *Structural optimization*, 17:1–13, 1999.
- [50] Rommel G. Regis and Christine A. Shoemaker. Improved strategies for radial basis function methods for global optimization. *J. of Global Optimization*, 37(1):113–135, January 2007. ISSN 0925-5001. doi: 10.1007/s10898-006-9040-1. URL <https://doi.org/10.1007/s10898-006-9040-1>.
- [51] Rommel G. Regis and Christine A. Shoemaker. Parallel radial basis function methods for the global optimization of expensive functions. *European Journal of Operational Research*, 182(2):514–535, 2007. ISSN 0377-2217. doi: <https://doi.org/10.1016/j.ejor.2006.08.040>. URL <https://www.sciencedirect.com/science/article/pii/S0377221706008800>.
- [52] Roman Garnett. *Bayesian Optimization*. Cambridge University Press, 2023.
- [53] Bobak Shahriari, Kevin Swersky, Ziyu Wang, Ryan P. Adams, and Nando de Freitas. Taking the human out of the loop: A review of bayesian optimization. *Proceedings of the IEEE*, 104(1):148–175, 2016.
- [54] Carl Edward Rasmussen and Christopher K. I. Williams. *Gaussian Processes for Machine Learning*. MIT Press, 2006.
- [55] Harold J. Kushner. A new method of locating the maximum point of an arbitrary multipeak curve in the presence of noise. *Journal of Basic Engineering*, 86(1):97–106, 1964.
- [56] Jonas Moćkus. On bayesian methods for seeking the extremum and their application. In *Optimization Techniques IFIP Technical Conference Novosibirsk*, pages 400–404. Springer Berlin Heidelberg, 1975.
- [57] Philipp Hennig and Christian J. Schuler. Entropy search for information-efficient global optimization. *Journal of Machine Learning Research*, 13(6):1809–1837, 2012.
- [58] Lukas P. Fröhlich, Edgar D. Klenske, Julia Vinogradska, Christian Daniel, and Melanie N. Zeilinger. Noisy-input entropy search for efficient robust bayesian optimization. In *Proceedings of the 23rd International Conference on Artificial Intelligence and Statistics*, volume 108, 2020.

- [59] Jian Wu and Peter I. Frazier. The parallel knowledge gradient method for batch bayesian optimization. In *Proceedings of the 30th International Conference on Neural Information Processing Systems*, page 3134–3142, Red Hook, NY, USA, 2016.
- [60] Zi Wang, Clement Gehring, Pushmeet Kohli, and Stefanie Jegelka. Batched large-scale bayesian optimization in high-dimensional spaces. In *Proceedings of the Twenty-First International Conference on Artificial Intelligence and Statistics*, volume 84 of *Proceedings of Machine Learning Research*, pages 745–754, 2018.
- [61] ChangYong Oh, Efstratios Gavves, and Max Welling. BOCK : Bayesian optimization with cylindrical kernels. In *Proceedings of the 35th International Conference on Machine Learning*, volume 80 of *Proceedings of Machine Learning Research*, pages 3868–3877. PMLR, 2018.
- [62] Amin Nayebi, Alexander Munteanu, and Matthias Poloczek. A framework for Bayesian optimization in embedded subspaces. In *Proceedings of the 36th International Conference on Machine Learning*, volume 97 of *Proceedings of Machine Learning Research*, pages 4752–4761. PMLR, 2019.
- [63] Yihang Shen and Carl Kingsford. Computationally efficient high-dimensional bayesian optimization via variable selection. In *Proceedings of the Second International Conference on Automated Machine Learning*, volume 224, pages 1–27, 2023.
- [64] David Eriksson, Michael Pearce, Jacob R. Gardner, Ryan Turner, and Matthias Poloczek. Scalable global optimization via local bayesian optimization. In *Proceedings of the 33rd International Conference on Neural Information Processing Systems*, volume 493, page 5496–5507, 2019.
- [65] David Eriksson and Matthias Poloczek. Scalable constrained bayesian optimization. In *Proceedings of the 24th International Conference on Artificial Intelligence and Statistics (AISTATS)*, volume 130. PMLR, 2021.
- [66] Mickaël Binois and Nathan Wycoff. A survey on high-dimensional gaussian process modeling with application to bayesian optimization. *ACM Trans. Evol. Learn. Optim.*, 2(2), 2022.
- [67] James Bergstra, Rémi Bardenet, Yoshua Bengio, and Balázs Kégl. Algorithms for hyperparameter optimization. In *Proceedings of the 25th International Conference on Neural Information Processing Systems, NIPS’11*, page 2546–2554, Red Hook, NY, USA, 2011. Curran Associates Inc. ISBN 9781618395993.
- [68] Frank Hutter, Holger H. Hoos, and Kevin Leyton-Brown. Sequential model-based optimization for general algorithm configuration. In *Learning and Intelligent Optimization*, pages 507–523, 2011.
- [69] Jasper Snoek, Oren Rippel, Kevin Swersky, Ryan Kiros, Nadathur Satish, Narayanan Sundaram, Md. Mostofa Ali Patwary, Prabhat Prabhat, and Ryan P. Adams. Scalable bayesian optimization using deep neural networks. In *Proceedings of the 32nd International Conference on International Conference on Machine Learning*, volume 37, page 2171–2180. JMLR.org, 2015.

- [70] Samuel Kim, Peter Y. Lu, Charlotte Loh, Jamie Smith, Jasper Snoek, and Marin Soljačić'. Deep learning for bayesian optimization of scientific problems with high-dimensional structure. *arXiv*, abs/2104.11667, 2022.
- [71] Eric Brochu, Vlad M. Cora, and Nando de Freitas. A tutorial on bayesian optimization of expensive cost functions, with application to active user modeling and hierarchical reinforcement learning. *arXiv*, abs/1012.2599, 2010.
- [72] Neil Houlsby, Ferenc Huszár, Zoubin Ghahramani, and Máté Lengyel. Bayesian active learning for classification and preference learning. *ArXiv*, abs/1112.5745, 2011. URL <https://api.semanticscholar.org/CorpusID:13612582>.
- [73] D. Wang and Y. Shang. A new active labeling method for deep learning. In *Proc. of IJCNN*, pages 112–119, 2014.
- [74] Michael Bloodgood. Support vector machine active learning algorithms with query-by-committee versus closest-to-hyperplane selection. In *IEEE International Conference on Semantic Computing*, pages 148–155, 2018.
- [75] W. Li, G. Dasarathy, K. N. Ramamurthy, and V. Berisha. Finding the homology of decision boundaries with active learning. In *Advances in Neural Information Processing Systems*, page 8355–8365, 2020.
- [76] Keze Wang, Dongyu Zhang, Ya Li, Ruimao Zhang, and Liang Lin. Cost-effective active learning for deep image classification. *IEEE Transactions on Circuits and Systems for Video Technology*, 27(12):2591–2600, 2017. doi: 10.1109/TCSVT.2016.2589879.
- [77] Hiranmayi Ranganathan, Hemanth Venkateswara, Shayok Chakraborty, and Sethuraman Panchanathan. Deep active learning for image classification. In *IEEE International Conference on Image Processing*, pages 3934–3938, 2017. doi: 10.1109/ICIP.2017.8297020.
- [78] Lin Yang, Yizhe Zhang, Jianxu Chen, Siyuan Zhang, and Danny Z Chen. Suggestive annotation: A deep active learning framework for biomedical image segmentation. In *International conference on medical image computing and computer-assisted intervention*, pages 399–407. Springer, 2017.
- [79] Balaji Lakshminarayanan, Alexander Pritzel, and Charles Blundell. Simple and scalable predictive uncertainty estimation using deep ensembles. In *Proceedings of the 31st International Conference on Neural Information Processing Systems, NIPS'17*, page 6405–6416, 2017.
- [80] William H Beluch, Tim Genewein, Andreas Nürnberger, and Jan M Köhler. The power of ensembles for active learning in image classification. In *Proceedings of the IEEE Conference on Computer Vision and Pattern Recognition*, pages 9368–9377, 2018.
- [81] Aditya Siddhant and Zachary C Lipton. Deep bayesian active learning for natural language processing: Results of a large-scale empirical study. *arXiv preprint*, abs/1808.05697, 2018.
- [82] Toan Tran, Thanh-Toan Do, Ian D. Reid, and G. Carneiro. Bayesian generative active deep learning. In *International Conference on Machine Learning*, 2019. URL <https://api.semanticscholar.org/CorpusID:135466220>.

- [83] Yoon-Yeong Kim, Kyungwoo Song, JoonHo Jang, and Il-chul Moon. Lada: Look-ahead data acquisition via augmentation for deep active learning. In M. Ranzato, A. Beygelzimer, Y. Dauphin, P.S. Liang, and J. Wortman Vaughan, editors, *Advances in Neural Information Processing Systems*, volume 34, pages 22919–22930. Curran Associates, Inc., 2021.
- [84] J. Sun, H. Zhai, O. Saisho, and S. Takeuchi. Beam search optimized batch bayesian active learning. In *Proceedings of the AAAI Conference on Artificial Intelligence*, volume 37, pages 6084–6091, 2023.
- [85] Binhui Xie, Longhui Yuan, Shuang Li, Chi Harold Liu, Xinjing Cheng, and Guoren Wang. Active learning for domain adaptation: An energy-based approach. In *Proc. of AAAI*, page 8708–8716, 2022.
- [86] S. Chakraborty, V. Balasubramanian, Q. Sun, S. Panchanathan, and J. Ye. Active batch selection via convex relaxations with guaranteed solution bounds. *IEEE Trans. Pattern Anal. Mach. Intell.*, 37:1945–1958, 2015.
- [87] Ozan Sener and Silvio Savarese. Active learning for convolutional neural networks: A core-set approach. In *International Conference on Learning Representations*, 2018. URL <https://openreview.net/forum?id=H1aIuk-RW>.
- [88] Y. Zhao, Z. Shi, J. Zhang, D. Chen, and L. Gu. A novel active learning framework for classification: Using weighted rank aggregation to achieve multiple query criteria. *Pattern Recognition*, 93:581–602, 2019.
- [89] C. Li, H. Ma, Z. Kang, Y. Yuan, X.-Y. Zhang, , and G. Wang. On deep unsupervised active learning. In *Proc. 29th Int. Joint Conf. Artif. Intell.*, page 2626–2632, 2020.
- [90] M. Hasan, S. Paul, A. I. Mourikis, and A. K. Roy-Chowdhury. Context-aware query selection for active learning in event recognition. *IEEE Trans. Pattern Anal. Mach. Intell.*, 42:554–567, 2020.
- [91] Cody Coleman, Edward Chou, Julian Katz-Samuels, Sean Culatana, Peter Bailis, Alexander C. Berg, Robert Nowak, and I. Zeki Yalniz Roshan Sumbaly, Matei Zaharia. Similarity search for efficient active learning and search of rare concepts. In *Proceedings of the AAAI Conference on Artificial Intelligence*, page 804–812, 2022.
- [92] D. Gudovskiy, A. Hodgkinson, T. Yamaguchi, and S. Tsukizawa. Deep active learning for biased datasets via fisher kernel self-supervision. In *Proc. IEEE/CVF Conf. Comput. Vis. Pattern Recognit. (CVPR)*, pages 9038–9046, 2020.
- [93] Y. Kim and B. Shin. In defense of core-set: A density-aware coresets selection for active learning. In *Proc. 28th ACM SIGKDD Conf. Knowl. Discovery Data Mining*, page 804–812, 2022.
- [94] Q. Jin, M. Yuan, Q. Qiao, and Z. Song. One-shot active learning for image segmentation via contrastive learning and diversity-based sampling. *Knowl.-Based Syst.*, 241, 2022.
- [95] S. Li, J. M. Phillips, X. Yu, R. M. Kirby, and S. Zhe. Batch multifidelity active learning with budget constraints. In *Proceedings of Advances in Neural Information Processing Systems*, page 995–1007, 2022.

- [96] A. Parvaneh, E. Abbasnejad, D. Teney, R. Haffari, A. Van Den Hengel, and J. Q. Shi. Active learning by feature mixing. In *Proc. IEEE/CVF Conf. Comput. Vis. Pattern Recognit. (CVPR)*, page 12227–12236, 2022.
- [97] P. Donmez, J. Carbonell, and P. N. Bennett. Dual strategy active learning. In *Proceedings of European Conference on Machine Learning*, page 116–127, 2007.
- [98] Changchang Yin, Buyue Qian, Shilei Cao, Xiaoyu Li, Jishang Wei, Qinghua Zheng, and Ian Davidson. Deep similarity-based batch mode active learning with exploration-exploitation. In Vijay Raghavan, Srinivas Aluru, George Karypis, Lucio Miele, and Xindong Wu, editors, *2017 IEEE International Conference on Data Mining*, pages 575–584, 2017.
- [99] Fedor Zhdanov. Diverse mini-batch active learning. *arXiv preprint arXiv:1901.05954*, 2019.
- [100] Samarth Sinha, Sayna Ebrahimi, and Trevor Darrell. Variational adversarial active learning. *2019 IEEE/CVF International Conference on Computer Vision (ICCV)*, pages 5971–5980, 2019. URL <https://api.semanticscholar.org/CorpusID:90258881>.
- [101] Jordan T. Ash, Chicheng Zhang, Akshay Krishnamurthy, John Langford, and Alekh Agarwal. Deep batch active learning by diverse, uncertain gradient lower bounds. In *International Conference on Learning Representations*, 2020.
- [102] Changjian Shui, Fan Zhou, Christian Gagné, and Boyu Wang. Deep active learning: Unified and principled method for query and training. In Silvia Chiappa and Roberto Calandra, editors, *The 23rd International Conference on Artificial Intelligence and Statistics*, volume 108 of *Proceedings of Machine Learning Research*, pages 1308–1318, 2020.
- [103] Gui Citovsky, Giulia DeSalvo, Claudio Gentile, Lazaros Karydas, Anand Rajagopalan, Afshin Rostamizadeh, and Sanjiv Kumar. Batch active learning at scale. In *Proceedings of Advances in Neural Information Processing Systems*, page 11933–11944, 2021.
- [104] B. Gu, Z. Zhai, C. Deng, and H. Huang. Efficient active learning by querying discriminative and representative samples and fully exploiting unlabeled data. *IEEE Trans. Neural Netw. Learn. Syst.*, 32:4111–4122, 2021.
- [105] S. Huang, T. Wang, H. Xiong, J. Huan, and D. Dou. Semi-supervised active learning with temporal output discrepancy. In *Proc. IEEE/CVF Int. Conf. Comput. Vis. (ICCV)*, pages 3447–3456, 2021.
- [106] Y. Geifman and R. El-Yaniv. Deep active learning with a neural architecture search. In *Proceedings of Advances in Neural Information Processing Systems*, page 5974–5984, 2019.
- [107] Jordan Ash, Surbhi Goel, Akshay Krishnamurthy, and Sham Kakade. Gone fishing: Neural active learning with fisher embeddings. In *Advances in neural information processing systems*, volume 34, 2021.
- [108] Akanksha Saran, Safoora Yousefi, Akshay Krishnamurthy, John Langford, and Jordan T. Ash. Streaming active learning with deep neural networks. *arXiv*, abs/2303.02535, 2023.

- [109] Greg Schohn and David Cohn. Less is more: Active learning with support vector machines. In *Proceedings of the Seventeenth International Conference on Machine Learning*, pages 839–846, 2000.
- [110] D. Roth and K. Small. Margin-based active learning for structured output spaces. In *Proc. Eur. Conf. Mach. Learn.*, page 413–424, 2006.
- [111] Burr Settles, Mark Craven, and Soumya Ray. Multiple-instance active learning. In John C. Platt, Daphne Koller, Yoram Singer, and Sam T. Roweis, editors, *Advances in Neural Information Processing Systems 20*, pages 1289–1296, 2007.
- [112] Nicholas Roy and Andrew McCallum. Toward optimal active learning through monte carlo estimation of error reduction. In *International Conference on Machine Learning*, page 441–448, 2001.
- [113] Alexander Freytag, Erik Rodner, and Joachim Denzler. Selecting influential examples: Active learning with expected model output changes. In *Computer Vision - ECCV*, volume 8692, pages 562–577, 2014.
- [114] Freddie Bickford Smith, Andreas Kirsch, Sebastian Farquhar, Yarin Gal, Adam Foster, and Tom Rainforth. Prediction-oriented bayesian active learning. In *International Conference on Artificial Intelligence and Statistics (AISTATS)*, 2023.
- [115] Nitish Srivastava, Geoffrey Hinton, Alex Krizhevsky, Ilya Sutskever, and Ruslan Salakhutdinov. Dropout: A simple way to prevent neural networks from overfitting. *Journal of Machine Learning Research*, 15(56):1929–1958, 2014. URL <http://jmlr.org/papers/v15/srivastava14a.html>.
- [116] Yarin Gal and Zoubin Ghahramani. Dropout as a bayesian approximation: Representing model uncertainty in deep learning. In Maria Florina Balcan and Kilian Q. Weinberger, editors, *Proceedings of The 33rd International Conference on Machine Learning*, volume 48 of *Proceedings of Machine Learning Research*, pages 1050–1059, New York, New York, USA, 20–22 Jun 2016. PMLR. URL <https://proceedings.mlr.press/v48/gal16.html>.
- [117] Chuan Guo, Geoff Pleiss, Yu Sun, and Kilian Q. Weinberger. On calibration of modern neural networks. In *Proceedings of the 34th International Conference on Machine Learning - Volume 70*, ICML’17, page 1321–1330. JMLR.org, 2017.
- [118] Moloud Abdar, Farhad Pourpanah, Sadiq Hussain, Dana Rezazadegan, Li Liu, Mohammad Ghavamzadeh, Paul Fieguth, Xiaochun Cao, Abbas Khosravi, U Rajendra Acharya, et al. A review of uncertainty quantification in deep learning: Techniques, applications and challenges. *Information Fusion*, 2021.
- [119] R Dennis Cook. Detection of influential observation in linear regression. *Technometrics*, 19(1):15–18, 1977.
- [120] R Dennis Cook and Sanford Weisberg. Characterizations of an empirical influence function for detecting influential cases in regression. *Technometrics*, 22(4):495–508, 1980.

- [121] R Dennis Cook. Assessment of local influence. *Journal of the Royal Statistical Society: Series B (Methodological)*, 48(2):133–155, 1986.
- [122] Pang Wei Koh, Kai-Siang Ang, Hubert HK Teo, and Percy Liang. On the accuracy of influence functions for measuring group effects. *arXiv preprint*, abs:1905.13289, 2019.
- [123] Han Guo, Nazneen Fatema Rajani, Peter Hase, Mohit Bansal, and Caiming Xiong. Fastif: Scalable influence functions for efficient model interpretation and debugging. *arXiv preprint*, abs/2012.15781, 2020.
- [124] Samyadeep Basu, Philip Pope, and Soheil Feizi. Influence functions in deep learning are fragile. *arXiv*, abs/2006.14651, 2020.
- [125] Samyadeep Basu, Xuchen You, and Soheil Feizi. On second-order group influence functions for black-box predictions. In *International Conference on Machine Learning*, pages 715–724. PMLR, 2020.
- [126] Xiaochuang Han, Byron C Wallace, and Yulia Tsvetkov. Explaining black box predictions and unveiling data artifacts through influence functions. *arXiv preprint*, abs/2005.06676, 2020.
- [127] Vitaly Feldman and Chiyuan Zhang. What neural networks memorize and why: Discovering the long tail via influence estimation. *arXiv preprint*, abs/2008.03703, 2020.
- [128] Marc-Etienne Brunet, Colleen Alkalay-Houlihan, Ashton Anderson, and Richard Zemel. Understanding the origins of bias in word embeddings. In *International Conference on Machine Learning*, pages 803–811. PMLR, 2019.
- [129] Zhuoming Liu, Hao Ding, Huaping Zhong, Weijia Li, Jifeng Dai, and Conghui He. Influence selection for active learning. In *Proceedings of the IEEE/CVF International Conference on Computer Vision (ICCV)*, 2021.
- [130] Meng Xia and Ricardo Henao. Reliable active learning via influence functions. *Transactions on Machine Learning Research*, 2023.
- [131] Victor Picheny, Tobias Wagner, and David Ginsbourger. A benchmark of kriging-based infill criteria for noisy optimization. *Structural and Multidisciplinary Optimization*, 48, 2013.
- [132] Alex Krizhevsky. Learning multiple layers of features from tiny images, 2009.
- [133] Kaiming He, X. Zhang, Shaoqing Ren, and Jian Sun. Identity mappings in deep residual networks. In *European Conference on Computer Vision*, 2016.

Supplementary Material

A Deriving the Jacobian of minimizer w.r.t. parameters

By definition of $\hat{x}_\theta^* =: \hat{x}_{\min}(\theta)$, the first-order condition is

$$0 = \nabla_x \mathbb{E}_{y \sim p_\theta(\cdot|x)}[y | x] \Big|_{x=\hat{x}_{\min}(\theta)} = \nabla_x A'(\eta_\theta(x)) \Big|_{x=\hat{x}_{\min}(\theta)}. \quad (43)$$

Define

$$g(\theta, x) := \nabla_x A'(\eta_\theta(x)) \in \mathbb{R}^{d_x}.$$

Then $g(\theta, \hat{x}_{\min}(\theta)) = 0$. Fix $\hat{\theta}_t$ and perturb $\theta = \hat{\theta}_t + \delta$ with

$$\Delta x := \hat{x}_{\min}(\hat{\theta}_t + \delta) - \hat{x}_{\min}(\hat{\theta}_t).$$

A first-order Taylor expansion gives

$$\begin{aligned} 0 &= g(\hat{\theta}_t + \delta, \hat{x}_{\min}(\hat{\theta}_t + \delta)) \\ &\approx g(\hat{\theta}_t, \hat{x}_{\min}(\hat{\theta}_t)) + \left[\frac{\partial}{\partial \theta} g(\theta, x) \right]_{\theta=\hat{\theta}_t, x=\hat{x}_{\min}(\hat{\theta}_t)} \delta + \left[\frac{\partial}{\partial x} g(\theta, x) \right]_{\theta=\hat{\theta}_t, x=\hat{x}_{\min}(\hat{\theta}_t)} \Delta x. \end{aligned}$$

Since $g(\hat{\theta}_t, \hat{x}_{\min}(\hat{\theta}_t)) = 0$, we obtain

$$\left[\frac{\partial}{\partial x} g(\theta, x) \right] \Delta x = - \left[\frac{\partial}{\partial \theta} g(\theta, x) \right] \delta,$$

hence

$$\Delta x = - \left[\frac{\partial}{\partial x} g(\theta, x) \right]^{-1} \left[\frac{\partial}{\partial \theta} g(\theta, x) \right] \delta \Big|_{\theta=\hat{\theta}_t, x=\hat{x}_{\min}(\hat{\theta}_t)}.$$

Noting that $\frac{\partial}{\partial x} g(\theta, x) = \nabla_x^2 A'(\eta_\theta(x))$, this becomes

$$\hat{x}_{\min}(\hat{\theta}_t + \delta) - \hat{x}_{\min}(\hat{\theta}_t) = - \left[\nabla_x^2 A'(\eta_\theta(x)) \right]^{-1} \left[\frac{\partial}{\partial \theta} \nabla_x A'(\eta_\theta(x)) \right] \delta \Big|_{\theta=\hat{\theta}_t, x=\hat{x}_{\min}(\hat{\theta}_t)}.$$

Sending $\delta \rightarrow 0$ yields the Jacobian (total derivative)

$$\frac{\partial \hat{x}_{\min}(\theta)}{\partial \theta} = - \left[\nabla_x^2 A'(\eta_\theta(x)) \right]^{-1} \left[\frac{\partial}{\partial \theta} \nabla_x A'(\eta_\theta(x)) \right] \Big|_{x=\hat{x}_{\min}(\theta)}.$$

B Experiment datasets

B.1 Noisy black-box function

2D Branin. The first function is the Branin function $f(\mathbf{x}) = a[(x_2 - bx_1^2 + cx_1 - r)^2 + s(1 - t) \cos(x_1) - q]$ where $a = 1/51.95$, $b = 5.1/(4\pi)^2$, $c = 5/\pi$, $r = 6$, $s = 10$, $t = 1/(8\pi)$ and $q = 44.81$, a rescaled form by [131]. The function is evaluated on the square $x_1 \in [0., 1.]$, $x_2 \in [0., 1.]$. It has three global minima $f(\mathbf{x}^*) = -1.0474$.

2D Drop-Wave function. This two-dimensional, radially symmetric test function is highly multimodal due to its oscillatory cosine term. For $\mathbf{x} = (x_1, x_2)$ it is defined as

$$f(\mathbf{x}) = -\frac{1 + \cos(12\sqrt{x_1^2 + x_2^2})}{0.5(x_1^2 + x_2^2) + 2},$$

and is typically evaluated on $x_i \in [-5.12, 5.12]$. It attains the global minimum $f(\mathbf{x}^*) = -1$ at $\mathbf{x}^* = (0, 0)$.

5D Ackley function. The Ackley function is generally expressed in the form $f(x) = -a \exp(-b\sqrt{\frac{1}{d} \sum_i x_i^2}) - \exp(\frac{1}{d} \sum_i \cos(cx_i)) + a + \exp(1)$, where $a = 20$, $b = 0.2$, $c = 2\pi$ and $\sigma = 0.5$. For the *dimension* $d = 2$, the function leads some optimization algorithms, particularly hill-climbing algorithms, to be trapped in one of its many local minima. The function is evaluated on the hypercube $x_i \in [-5, 5]$, for $i = 1, \dots, d$. We set the dimension $d = 5$ for higher dimensional analysis. The *Global minimum* $f(\mathbf{x}^*) = 0$ is achieved at $\mathbf{x}^* = (0, \dots, 0)$.

B.2 Hyperparameter tuning under distribution shift

We use CIFAR-10 [132], which contains 50,000 training images and 10,000 test images across 10 classes. The predictive model is a Pre-Activation Residual Network [133]. We construct a target (unlabeled) evaluation set by selecting 3,000 CIFAR-10 test images whose (unknown-to-the-learner) labels belong to a restricted class set $C := \{C_1, C_2, C_3\}$ (1,000 images per class). We also construct a labeled source dataset (X, Y) that is deliberately imbalanced: it contains 500 labeled instances from each class in C , and 5,000 labeled images from each of the remaining classes in $Y \setminus C$. Hyperparameter acquisition methods are evaluated by their impact on performance on the target subset, while training leverages the labeled source data.

B.3 Predictive learning

B.3.1 MNIST active learning benchmark

MNIST [40] contains 60,000 training images and 10,000 test images over 10 digit classes. Following [44], we initialize the active learning loop with a random but class-balanced labeled set of 20 points (two per class). We hold out 1,024 training points as a validation set; the remaining training points form the acquisition pool. Test accuracy is reported on the standard MNIST test set after each acquisition step.

B.3.2 EMNIST Letters active learning

EMNIST Letters [41] is a balanced 26-class character recognition task with 124,800 training images and 20,800 test images. We set aside the last portion of the training set—equal in size to the test set—as a validation set, and use the remaining training points as the acquisition pool. We follow the same pool-based acquisition loop as in MNIST, starting from a small randomly initialized labeled set.

B.3.3 Rotten Tomatoes movie-review phrases

We evaluate binary sentiment classification using the Rotten Tomatoes phrase dataset originally collected by Pang and Lee [48]. The original labels are ordinal with five levels (“negative”, “somewhat negative”, “neutral”, “somewhat positive”, “positive”). To construct a binary task, we remove neutral phrases, map {“negative”, “somewhat negative”} to 0 and {“somewhat positive”, “positive”} to 1, and then randomly split the resulting dataset into 59,070 training phrases, 1,024 validation phrases, and 16,384 test phrases. For text preprocessing, we use a bag-of-words representation; we discard words with total occurrence less than 10, reducing the feature dimension from 15,186 to 7,004.